University of Algarve

Study of the backscattered ultrasound energy for invasive tissue temperature estimation

Javid Jalilzadeh Rahmati

Dissertation of

Integrated Master in Electronics and Telecommunication Engineering

Faculty of Science and Technology

Supervised by

Maria da Graça Cristo dos Santos Lopes Ruano

2012

Universidade do Algarve

Estudo da energia de ultra-som para a estimativa de retro-espalhamento invasiva em tecidos mediante temperatura

Javid Jalilzadeh Rahmati

Dissertação de

Mestrado Integrado em Engenharia Eletrónica e Telecomunicações

Faculdade de Ciências e Tecnologia

Trabalho efetuado sob a orientação de:

Maria da Graça Cristo dos Santos Lopes Ruano

2012

“Logic will get you from A to B.

Imagination will take you everywhere.”

Albert Einstein

1879-1955

Declaração da Autoria do trabalho

Declaro ser o autor deste trabalho, que é original e inédito. Autores e trabalhos consultados estão devidamente citados no texto e constam da listagem de referências incluída.

Declaration of Authorship of work

I hereby declare that, I am the author of this work, which is original and unpublished. Authors and works consulted are properly cited in the text and included in the list of references included.

Resumo

Este trabalho experimental enquadra-se na aplicação de ultrassom para hipertermia (terapêutica térmica) com vista ao tratamento de células neoplásicas. A análise da energia do ultrassom retro-difundida possibilita o estudo do comportamento da variação de temperatura espalhada pelo sinal ultrassónico nos tecidos, constituindo o objetivo primordial deste trabalho. Para a realização das experiências foram desenvolvidos 'phantoms' baseados em agar-agar para mimificar o comportamento dos tecidos humanos com o ultrassom. Posteriormente, com vista a obter um 'phantom' mais próximo do tecido humano, as experiências foram repetidas com lombo de porco *ex-vivo*. As experiências envolveram instrumentação ultrassónica de terapêutica e de imagem, conectados a instrumentação de geração de funções e de aquisição de sinais. Foram realizadas experiências considerando diferentes energias (0.5, 1, 1.5 e 2 W/cm3) do transdutor de terapia e duas frequências de emissão do transdutor de imagem (5 e 7 MHz). Utilizaram-se 5 sensores de temperatura para medição invasiva da temperatura nos fantômas baseados em gel e dois sensores nas experiências com lombo de porco. Analisando os atrasos temporais nos ecos dos sinais ultrassónicos retro-espalhados para ambos os tipos de 'phantoms' verificou-se a relação entre o aumento de temperatura e o aumento da velocidade de propagação dos ecos. A análise das variações das energias retro-espalhadas provou ser dependente da temperatura aplicada no lombo de porco não sendo contudo conclusiva no caso dos 'phantoms' baseados em gel.

Palavras-chave: *Energia retro-espalhada, hipertermia, ultrassom, Estimação de temperatura*

Summary

This experimental work is part of the application of ultrasound for hyperthermia (thermal therapy) aiming at treatment of cancer cells. The analysis of the back-scattered ultrasound energy enables the study of the temperature behavior induced by the ultrasonic signal in the tissues and it is the primary goal of this case study. To carry out this experiment we developed a gel-based phantom which mimics the behavior of human tissues under ultrasound signals.

Subsequently, in order to obtain a more human like phantom the experiments were repeated with ex-vivo pork loin. The experiments involved ultrasonic therapeutic and imaging instrumentation connected to a function generator and a signal acquisition system. Experiments were performed considering different energies (0.5, 1, 1.5 and 2 W/cm^3) of the therapeutic transducer and two emission frequencies of the image transducer (5 and 7 MHz). Five temperature sensors were used to measure the invasive temperature in the gel-based phantoms and two sensors in the experiments with pork loin.

Analyzing the time delays in the echoes of the back-scattered ultrasonic signals of both types of phantoms we verified the relationship between temperature rise and the increase in the speed of propagation of the echoes.

The assessment of variations in the back-scattered energy proved its dependency on the temperature applied in pork loin tissue, but no conclusion could be taken in the case of gel-based phantom.

Keywords: *Backscattered Energy, Hyperthermia, Ultrasound, Temperature Estimation*

Acknowledgements

First of all, I wanted to thank my supervisor Prof. Dr. Maria Graça Cristo dos Santos Lopes Ruano for the initial invitation and the support and friendship throughout this integrated master thesis.

My respect and thanks to all colleagues in control and biomedical signal processing laboratory especially Eng. Behrooz Zabihian and Eng. Duarte Silva for their help and support which contributed to overcome the difficulties during this integrated master course.

Also wanted to thank my parents and my lovely wife, Atefeh Torkamani, for their limitless kindness to me.

At the end, I wanted to thank to all my friends in Faro's city for their support and help during this thesis project.

And Special thanks to pioneer scientists:

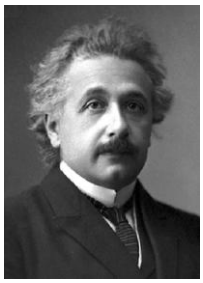

Albert Einstein
1879-1955

Max Gerson
1881-1959

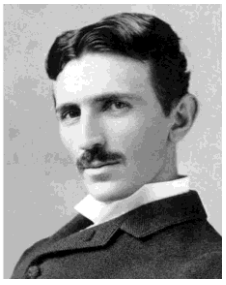

Nikola Tesla
1856-1943

William Nelson
1923-1996

Table of Contents

List of Figures

List of Tables

Chapter 01

Introduction

Chapter 1

Introduction

1.1 Motivation

Thermal therapy has been applied for thousands of years presenting a long history of being employed in ancient civilizations like Chinese and Roman. Thermal therapy has become one of the cutting edge issues in nowadays medical world since the treatment procedure involves low risk of side effects both during and after the medical application.
Ultrasound hyperthermia cancer treatment is the thermal therapy methodology which applies temperatures between 41 and 45ºC on tumors. The temperature is raised due to the interference of ultrasound with the tissues. It has been considered the leader therapy in terms of better impact on treating the cells which are supposed to be treated and maintaining the cells close to the cancer in comparison with other treatment techniques.
For the above mentioned reasons, a massive amount of researches have been investigating and are still in progress to find how to achieve the optimum efficiency in thermal therapies using the energy of ultrasound signals. [1]
In this thesis we tried to evaluate the variation of temperature in tissues by examining the effect of the ultrasound backscattered energy on temperature. This study aims to contribute on the field of ultrasound focused heating of a tissue area, the cancerous area, without affecting the surrounding cells.[1]

1.2 Proposed Goals

The major goal of this thesis is to develop experiments to evaluate ultrasound induced temperature variations in tissues. To achieve so phantoms should be used to perform the following issues:

- Analysis of the echo-shifts and energy of the backscattered ultrasound signals in relation with the temperature variations observed in phantoms;
- Evaluation of the procedure of temperature estimation by ultrasound backscattered energy analysis when ex-vivo pork loin is employed as a human-like tissue phantom.

1.3 Thesis Outlines

This thesis was organized according to the following chapters:

The present chapter gives a brief description of the motivation underlying this work and states the proposed goals of this thesis.

Chapter 2 describes the background knowledge required to pursue this work and the practical concepts requested for setting up the experiments.

Chapter 3 explains the experimental setup developed in all experiments, the instrumental tools employed and the steps required for completing the experiments.

Chapter 4 presents the results obtained during the experimental work complemented with the respective comments.

Finally Chapter 5 summarizes the achievements of this thesis and points out some research issues to be developed in the near future.

Chapter 02

Background

Chapter 2

Background

2.1 Introduction

The backbone information relevant for comprehending the applicability of ultrasound and in particular its usage in this thesis will be discussed in this chapter. The main physics of ultrasound as well as typical analysis of ultrasound signals will also be explained. Several books and scientific articles have been consulted related to these subjects but an effort was made towards a synthetic description of only the most relevant points.

2.2 Ultrasound general concept

Ultrasound, this is acoustic energy in the form of waves having a frequency above the human hearing range (above 20 kHz, or 20,000 periods per second), is frequently used in research and industrial applications.

Modern ultrasound devices can generate sound with frequencies of as greater as several GHz (up to about 10GHz have been achieved [2]) by transducing electrical power into mechanical oscillations. There may be a maximum to the consistency of deployment in ultrasound applications, but it is not yet known. However, the higher frequencies used in nowadays applications are challenging since they are not easy to generate and to evaluate. [2]

Production and detection of ultrasound signals is done mainly through the use of piezoelectric devices or by optical indicators. Study of ultrasound waves is possible because they are noticeable by the diffraction of light. In general people hear signals from 18 kHz to 20 kHz. However ultrasound presents frequencies much above these values. Some animals can listen to ultrasound, for example, bats and sharks, who understand

echoes arriving above 100 KHz. Ultrasonic waves, can be used in several applications and in this chapter we will group them into industrial and medical applications. [2]

Figure 2.1 presents a periodic ultrasonic wave which is obtained by an emitting source of ultrasound and its correspondent variation among the time. [3]

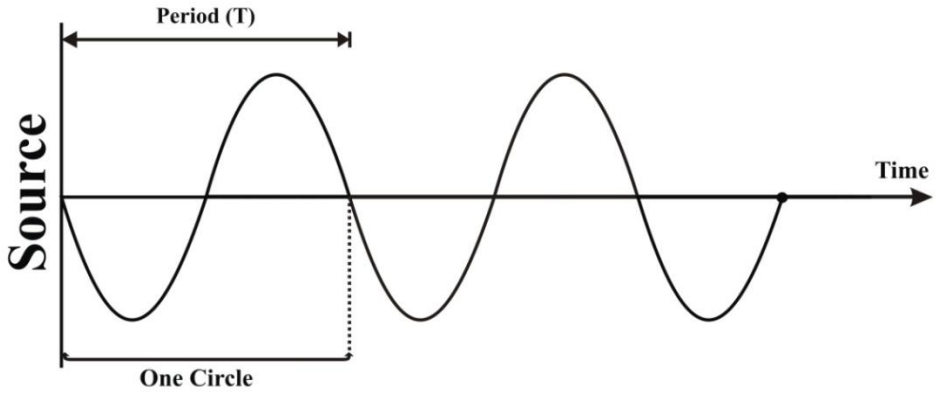

Figure 2.1: The continuous ultrasound wave source-surface location modifying with time. [3]

2.2.1 Industrial ultrasound applications

Ultrasound has a huge variety of applications in industry. Being impossible to describe them all and being out of scope of this thesis, only some of the main applications are described below.

Cleaning: It is probably the most frequently application. Ultrasound is used to remove fat, dust, corrosion and color from steel, clay, glass and several other materials of the parts used in electronics, vehicles, planes and laboratory cleaners. This washing method is achieved through the use of the ultrasound cavitation effect. By irradiating a medium with ultrasound signals some regions of the medium are all of a sudden compressed and others rarefied giving rise to gas bubbles. These bubbles enable cleaning. [2]

Machining: Another application of ultrasonic technological innovation is the machining of components. Ultrasound machining has the benefits over the traditional technical machining methods of being appropriate for producing uncommon or

complicated designs since no rotary tool is necessary. Among the components that can be so prepared are smooth precious metal, ceramics, wine glass and tungsten carbide. [2]

Soldering and Welding: Ultrasound has also become very useful in soldering and welding of components. In the situation of soldering, the cavitation created by intensified ultrasonic beam eliminates the oxide coating on steel, thus allowing components to be registered with tin soldering components without the use of flux. In ultrasound application in welding, pressure and heat created by the material vibratory of the content to be welded and an ultrasound welding allows a thick piece of steel to be welded to a much thicker area. Ultrasonic methods can furthermore be used to weld items of identical or distinct plastic material to each other. [2]

Electronics: Ultrasonic application is very well related to the electrical gadgets industry. One of the reasons is, of course, because ultrasound signals are produced, recognized and considered by this technology. Also, ultrasonic technology is substantially used for examining, cleaning and soldering the automated elements. In addition, SAW (surface sound wave) filter are a type of automated element which functions at ultrasound wavelengths. They are important for a growing range of gadgets productions, such as mobile phone devices and TV devices. [2]

Agriculture: Ultrasound has been employed to evaluate the width of fat levels on pigs and cows as part of animal's vitals and safety control. It has also been used to strengthen the quality of homogenized applications. A related application is insect control, such as eliminating insects. [2]

Oceanography: In addition to the monitoring of submarines, oceanographic applications include generating the shapes of the sea base, getting submerged delivers and in the search of educational institutions of species of fish. [2]

In the above we have just explained some of the most important application in industry and still there are an enormous amount of other ultrasound applications which are not mentioned.

2.2.2 Medical ultrasound applications

The ultrasound application in the healthcare industry has been engaged with diagnostic and therapy approaches. The diagnostic usage of ultrasound is essentially as a

medical imaging technique. It is applied to visualize internal organs and enable measuring their size and structure, and to evaluate the existence of pathological lesions. In this kind of applications the echoes of the ultrasound emitted signals are employed to reconstruct the anatomic structures under observation or to identify the direction of movement of body fluids.

In what concerns the application of ultrasound in therapy, cavitation, mechanical and temperature effects are the physical principles to be considered. [4]

In terms of therapeutic ultrasound modalities we should consider two main areas of medical ultrasound application which are physiotherapy, hyperthermia, surgery and tissue ablation. The physiotherapy application, generally includes injury treatment in soft tissue, acceleration of bone and wound recovery, and to reduce the joint stiffness. The piston-like transducer which is presented in figure 2.2 is the mostly applied in physiotherapeutic ultrasound devices.

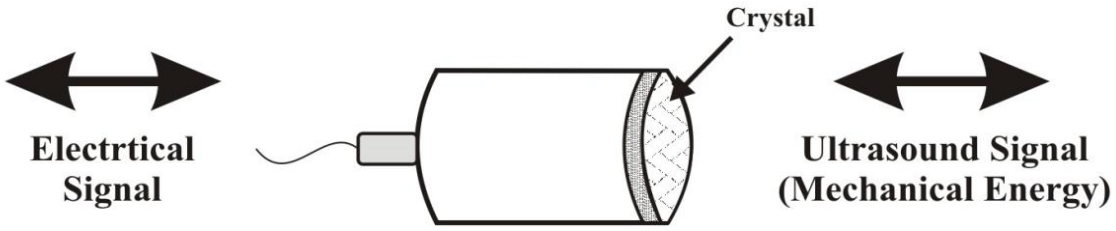

Figure 2.2: The piston-like transducer, generally applied on physiotherapy. [5]

Hyperthermia is a more recent application of the therapeutic ultrasound. It is mostly applied in cancer treatment, exclusively or in parallel with other techniques. The main factor of ultrasound hyperthermia is emitting the ultrasound beam focused on tumor or cancer cells at approximately 60 minutes and rising the temperature of the specific tissue between 43 and 45ºC. This beam can be generated by ordinary ultrasound transducers with lens, curved phase array transducers and acoustic mirror systems. The main problematic issue in this technique is when the beam is not focused or focused on other healthy cells around the cancerous cells, it will lead to damage of healthy cells rather than the affecting of cancerous cells. [5]

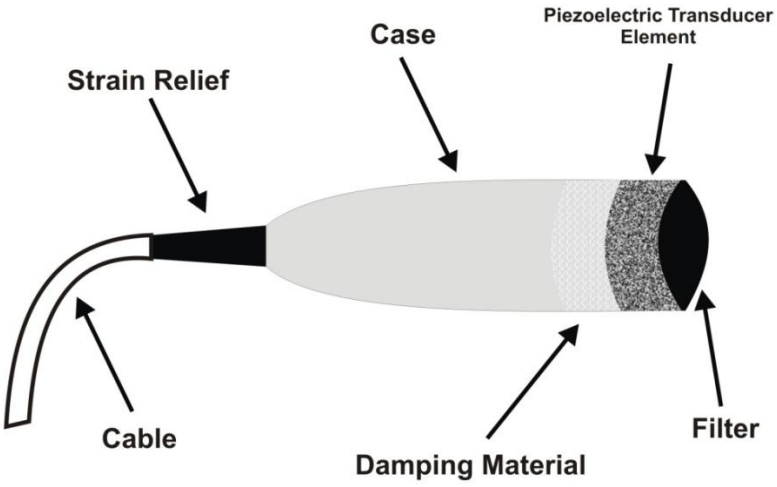

Figure 2.3: The ultrasound transducer and its parts (simple transducer). [6]

2.3 Effects of ultrasound propagation on media

During the propagation process of an ultrasound signal through a medium we will generally face the attenuation of the ultrasound beam in different procedures. The ultrasound beam will depart due to obstacles in the propagation mechanism such as refraction, reflection and scattering. Also absorption will be produced by conversion of the sound mechanical energy into heat. Approximately there is 1 dB cm^{-1} MHz^{-1} attenuation in ultrasound propagation into the soft tissue**.** [7]

2.3.1 Refraction

If there is two media with ordinary incidence of 90 degree and a wave is transmitting in borderline of these two media, the propagation will be without deviation components into the secondary media, the refraction will bent the wave at the oblique incidence. The related calculation defined by Snell's law: is

$$\frac{\sin \theta_i}{\sin \theta_t} = \frac{c_1}{c_2} \qquad (1)$$

In equation (1) where c_1 is the wave velocity in the first medium and c_2 represents the wave velocity in the secondary medium.

The bare eye cannot normally sense the refraction at the interface of two different tissues in the majority of the medical ultrasound images but it will be noticeable by using a simulated phantom.

2.3.2 Reflection

Reflection occurs when the ultrasound detents a border between two different media which is larger in comparison with the ultrasound wavelength. In these situations part of the energy is reflected back to the first medium and another part is transmitted to the second medium. And it is important to mention that the specular reflection has similar behavior to the optical reflection i.e., $\theta_i=\theta_r$.

In case of having normal incidence, the reflection will be in the same path of propagation and it will define the concept of echo type, the basis in the ultrasound echo imaging employed in medical diagnosis. Figure 2.4 depicts reflection.

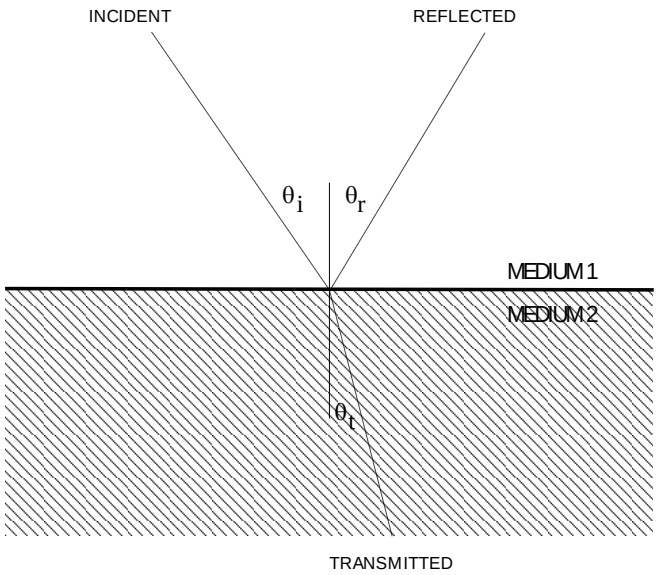

Figure 2.4: Reflection of a wave crossing two different media, where the incident angle is presented by θ_i , reflected angle θ_r and transmitted angle θ_t. [7]

To be also mentioned that the amount of reflected and transmitted energies depend on the acoustic impedance (Z) of the each media. Z is proportional to the density of the

medium (ρ) and to the speed of sound (c) in that particular medium – Z∝ ρ.c. The energy that is reflected at the interface of the two media is given by equation (2).

$$\frac{I_r}{I_i} = \left(\frac{Z_2 - Z_1}{Z_2 + Z_1} \right)^2 \quad (2)$$

I_r	intensity of reflected ultrasound
I_i	intensity of incident ultrasound
Z_1	acoustic impedance in medium 1
Z_2	acoustic impedance in medium 2

Where Ir and Ii are the intensities of the reflected and incident ultrasound, respectively Z1 and Z2 are the impedances of media 1 and 2 respectively.

Table 2.1 presents the values of the acoustic impedance of some materials and Table 2.2 the percentage of energies that are reflected according to some examples of pairs of media.

Table 2.1: Acoustic impedance of different materials. [7]

MATERIAL	Z (10^6 kg m^{-2} s^{-1})
AIR	0.0004
LUNG	0.26 – 0.46
BONE	3.75 – 7.38
WATER	1.52
LIVER	1.65
KIDNEY	1.62
BLOOD	1.61
FAT	1.38
TISSUE	1.35 – 1.68

Table 2.2: Percentage of energy that is reflected when ultrasound is travelling from first to second pair of media (left column). [7]

BOUNDARY	**% REFLECTED** at normal incidence
MUSCLE/BLOOD	0.07%
FAT/MUSCLE	1.08%
SOFT TISSUE/WATER	0.23%
SOFT TISSUE/AIR	99.9%
SOFT TISSUE/BONE	41.2%

According to equation (2), in the case of $Z_1=Z_2$ there is no reflected echoes and all the energy will be transmitted through the boundary between the media. But if there is a large difference between the two acoustic impedances approximately the whole wave will be reflected as echo and only a very small portion of wave energy will be transmitted. In medical applications of the ultrasound, this is normally not a problem because coupling gel is used on the surface of the skin to enable a better transmission of the signal energy to the inner body avoiding as so the air between the pair soft tissue /air.

2.3.3 Scattering

When there is a target under the ultrasound signal's pressure and it is small compared to the wavelength of then sound wave or is small and presents a rough surface, the object will re-radiate or scatter the sound signal's energy to the surroundings at an undesired order. If there is a large amount of scattering targets it will cause multiple scattering. For example, within blood the red blood cells constitute scatterers. An example of a single target scattering is presented in figure 2.5.

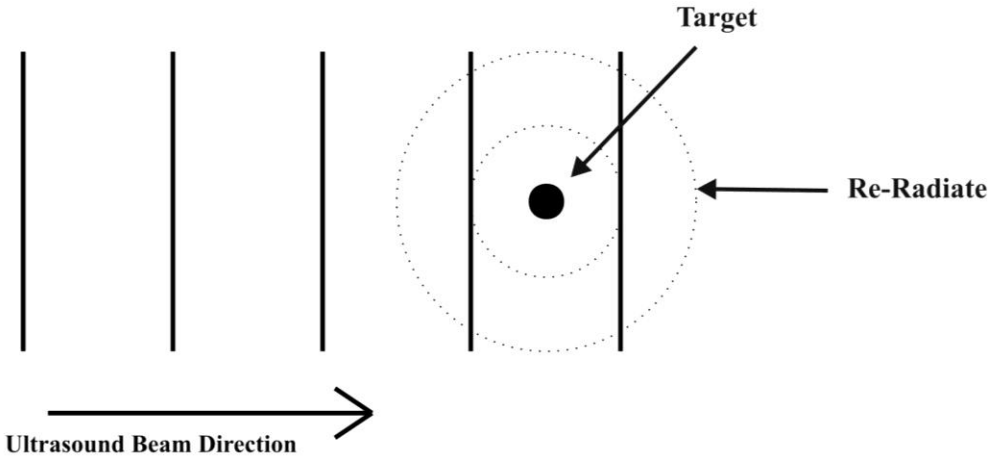

Figure 2.5: Ultrasound scattering caused by a small target (in comparison with the sound wave signal's wavelength). [7]

In figure 2.5, the scattered energies are acting as auxiliary sources of ultrasound since part of them re-radiate energy that is directed to the main source of ultrasound.

Nevertheless, the energy reflected from the medium boundaries is much higher than the scattered intensity. For instance, the scattered intensities observed from boundaries between fat/muscle and some body tissues are given in table 2.3.

Table 2.3: Ultrasound scattered energy between fat and muscle boundaries with body tissues (left column). [7]

Placenta	**-20dB (10^{-2})**
Liver	**-30dB (10^{-3})**
Kidney	**-40dB (10^{-4})**
Blood	**-60dB (10^{-6})**

2.3.4 Absorption

When the mechanical energy is converted into heat we describe the phenomena as absorption. In the case of soft tissues, above 90% of the total amount of attenuation is due to absorption.

There is an exponentially fall off with distance related to the absorption concept which is shown in figure 2.6.

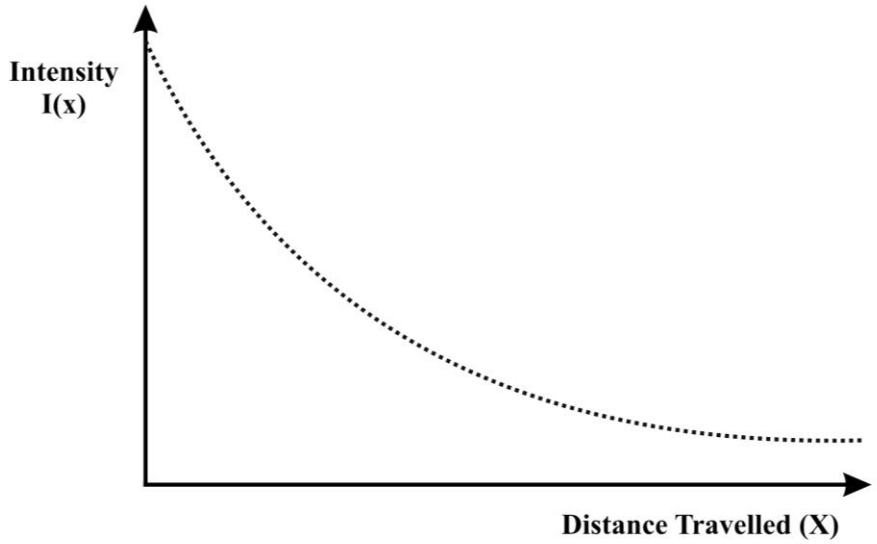

Figure 2.6: Dependence of intensity decrease due to absorption as function of the traveled distance. [9]

In figure 2.6 the exact value of intensity *I*, at a desired distance is given by equation (3)

$$I = I_0 \exp(-\mu_A x) \tag{3}$$

Where I_0 is the initial intensity at $x = 0$, μ_A is the intensity absorption coefficient and x represents the travelled distance.

In equation (3) the absorption coefficient μ_A is influenced by physical characteristics of the tissue and a function of the ultrasound signal frequency, so in this case when having less frequency we will have less attenuation percentage.

The more efficient approach is to instead define μ_A, as the half-value thickness amount of media thickness necessary to decrease the ultrasound intensity by 50% or -3dB.

Table 2.4: Half value thickness in centimeter for 2 and 5 MHz in different media. [7]

MATERIAL	2MHz	5MHz
Air	0.06	0.01
Bone	0.1	0.04
Water	340	54
Soft Tissue	2.1	0.86
Blood	8.5	3.0
Liver	1.5	0.5

As it is shown in table 2.4, the value of μ_A is smaller for air and bone. As seen in Table 2.1 these are media presenting stronger ultrasound reflections. To be also mentioned that they have also small attenuations [7].

2.4 Ultrasound instrumentation on practical experiments

After introducing the concept of ultrasound experiment should be performed based on an reliable experimental setup [8], described in detail in section 3.2.1.

2.5 Temperature estimation methods

To study the effects of ultrasound on medical applications there are, in general, four possible strategies: analysis of the ultrasound temporal echo-shifts, inspection of the variations in the signal's spectral content by tracking the frequency variations of the echoes, following the attenuation coefficient variations, and, analyzing the variations in the ultrasound backscattered energy signals. On this thesis we will concentrate on the analysis of both temporal echo-shifts and backscattered energy signals. To tackle these issues several methodologies have been proposed in literature. We present below some examples of these methods.

2.5.1 Ultrasound temporal Echo-shifts analysis methods

The ultrasound echoes have been addressed in different ways aiming at tissue temperature estimation.

The ultrasound statistical nature is due to the accumulation of randomly located back scatterings inside the tissue. The statistics analysis of the echoes may be analyzed to distinguish the logical relations between the echo images and the medium parameters. Under this approach authors focus on the first order statistical analysis for regular echo scattering conditions. Several possible analyzing procedures are available such as the Rayleigh distribution and its generalized forms and the K (introduced in [9]) and Rice distributions. But these methods do not have big functionality. The referred version of K distribution model is homodyne which combined a type of Rice distribution features and the K model for modeling and analyzing the statistics of the echo envelope. The mentioned investigations demonstrate that K distribution can also be applied on the variations of statistics of the echo envelope related to the modification in the number of scatterer density. The same author defined that the SNR (signal to noise ratio) can be applied for evaluation of statistical assets and measurement of scattered density.

In addition, one of the most important complications in clinical ultrasound analysis is the non-linearity of the signal which causes alterations in the statistics of the image acquired from the clinical examination. Furthermore, in the Dr. Vinayak Dutt's [9] thesis he examined the log compression involved in the signal processing for clinical

application and developed a image modeling methodology, the compressed images. Also he demonstrated that the variance of the compressed images have the same functionality as the scatterer density. [10]

Another methodology employed to estimate ultrasound induced temperature is to analyze the shifts occurred on the echoes. A group of researchers in Indiana University School of Medicine for analyzing the effect of ultrasound signal echo shifting in clinical thermal therapy application. The heated volume of medium is returning some time shifting in echoes when there is a clinical ultrasound application being processed. Here heat is produced by frequent triggering of a sharply focused high-intensity ultrasound signal emitting towards the tissue. By applying cross-correlation methods in transient variations among echoes, obtained at various temperatures, it is possible to estimate the temperature in dependence on the echo shift variations. For having a linear equation between echo time shift (delay) and temperature, studies demonstrated that spatial-peak temporal-peak intensities (ISPTP) of less than 950 W/cm^2 were required.

Also in case of approximately 10ºC rising in spatial peak temperature, there is more reliable and accurate temperature estimations. Furthermore due to nonlinear factors produced during high-intensity ultrasound signal emitting, no momentous influence was detected on the obtained delay. In case of having ISPTP of 1115-2698 W/Cm^2, the delay-temperature equation presents an analogous monotonically declining outline, but when the temperature is peaked its slope progressively increased. As conclusion, the results were completely fit into the theoretical predictions and inspire further experimental work to confirm other features of this methodology. [11]

Further studies in non-invasive hyperthermia at one dimension temperature estimation by temporal echo-shifts assessment can be found in [12].

2.5.2 Ultrasound back-scattered analysis methods

In this thesis we focused on localized hyperthermia, this is of the possible hyperthermia classifications as stated by S. Aida and K. Matsumoto [13].

Previous work of Dr. R. M. Arthur and his research partner [14], on focused hyperthermia assessment demonstrated that temperature can be evaluated by analysis of

the variations in back-scattered energy (BSE) from pulsed ultrasound with limited range. Furthermore, the expected variations in backscattered power were corresponded to the experimental in vitro conditions where bovine liver organ, chicken breasts, and chicken rib muscular tissue were employed.

In the same article, authors observed BSE variations with temperature in tissues with several scatterers, with different range of scatterers, and in selections of scatterers. In this article they assessed the BSE with a targeted rounded transducer of 7.5 MHz proving that BSE is a suitable parameter for temperature estimation although its accuracy and spatial resolution had not been established. Thus the use of the ultrasound BSE parameter for temperature estimation on artificial tissue's phantoms believed to be useful on the estimation of temperature in vivo tissues**.** [14]

The group of scientist from Washington University in a presentation which is described in [14] generates a procedure for creating the 3D temperature maps in homogeneous tissue. Temperature was measured by Arthur's group [14] noninvasively, quickly and at low cost with 0.5^{o}C of reliability and 1 cm^3 resolution.

By applying a single backscatter view and employing the standard equipment to find simple measurements for equation (4), we are able to calculate the power which is received from a tissue volume Sτ, where S is the beam area and τ is the duration of the emitting signal, assuming a lossless medium:

$$P_r(T) = \frac{2\,H^2\,\delta}{8\,R^4\,\alpha(T)}\,\eta(T)\,S\,(1 - e^{-2\alpha(T)c(T)\tau})\left[\frac{e^{\alpha(T)c(T)\delta} - e^{-\alpha(T)c(T)\delta}}{2\,\alpha(T)c(T)\delta}\right] \quad (4)$$

H and δ are the amplitude and duration of the insonifying burst, R is the distance from the transducer to the scattering volume, α(T) is the attenuation, c(T) is the speed of sound and η(T) is the backscattered coefficient applied to the scattering volume.

Furthermore, we can have the normalization process of backscattered energy to regular body temperature (37ºC), as in equation (5):

$$\eta(T)/\eta(37) = \frac{\left(\frac{\rho_m c(T)_m^2 - \rho_s c(T)_s^2}{\rho_s c(T)_s^2}\right)^2 + \frac{1}{3}\left(\frac{3\rho_s - 3\rho_m}{2\rho_s + \rho_m}\right)^2}{\left(\frac{\rho_m c(37)_m^2 - \rho_s c(37)_s^2}{\rho_s c(37)_s^2}\right)^2 + \frac{1}{3}\left(\frac{3\rho_s - 3\rho_m}{2\rho_s + \rho_m}\right)^2} \quad (5)$$

Where ρ is the density of the medium (m) or scatterer (s).The backscatter coefficient is given by the scattering cross section of a sub wavelength scatterer.

As a result, in terms of normalized backscattered energy, attenuation and speed of sound in liver (from Bamber and Hill (1979) as extracted by Haney and O'Brien (1986)) were applied for prediction of changes in backscattered energy (BSE). And they ended up with graphs of attenuation and velocity versus temperature as in figure 2.7.

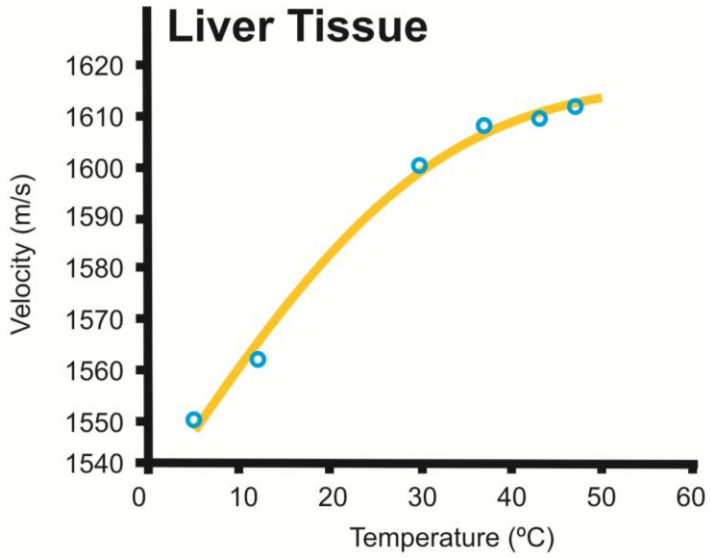

Figure 2.7: Temperature versus velocity on liver examination under ultrasound beam with 7MHz. [14]

In figure 2.7, polynomial fits (lines) of these and other data (circles) were used to predict the effect of attenuation and backscatter coefficient on the backscattered power level. And also following figure 2.7 another measurement has been made for prediction of temperature by backscattered energy values, which is presented in figure 2.8.

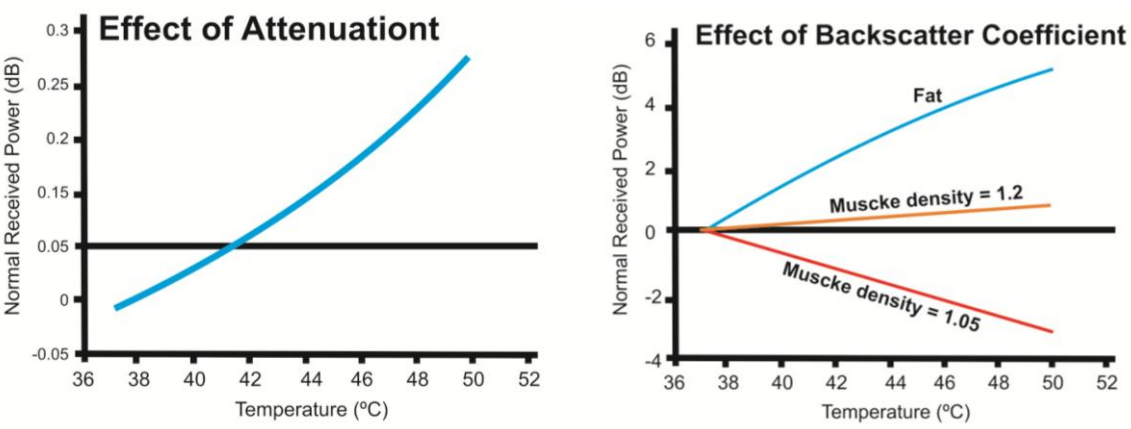

(a) *(b)*

Figure 2.8: (a) Effect of attenuation in terms of normalized received power (dB) on the temperature,(b) effect of backscattered coefficient in term of a relation between normalized received power (dB) and temperature (Cº). [14]

In figure 2.8, measured changes in backscattered energy (BSE) from temperatures varying from 37 to 50ºC were consistent with the authors' model [14] of the energy reflected from sub-wavelength scatterers. Since this approach exploits inhomogeneities present in tissue, if it is successful in vitro, it is expected that it will also hold for in vivo application. There is example of raw presentation of the BSE variation versus temperature in figure 2.9. [14]

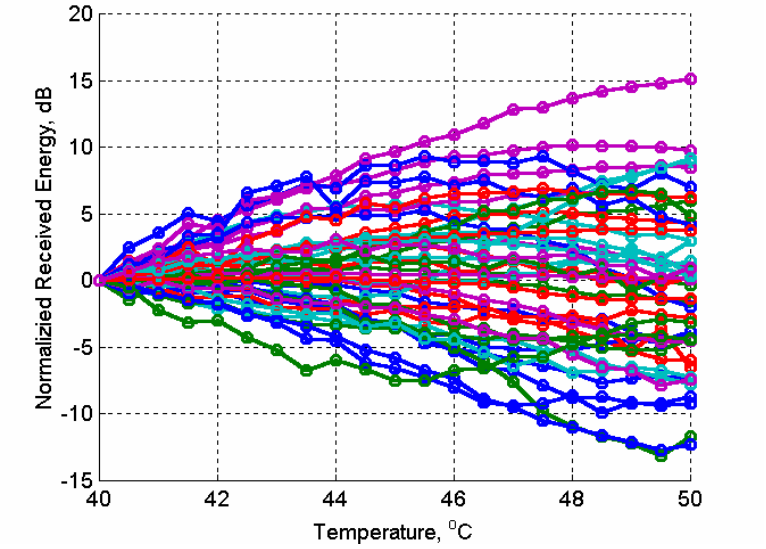

Figure 2.9: BSE versus temperature related of different types of tissues under the emitting ultrasound. [14]

Chapter 03

Experimental Setup

Chapter 3

Experimental Setup

3.1 Introduction

The experimental setup developed for this particular case study contains different devices and several operating conditions hereby described. The gel-based and the human-like tissues used as phantoms on the experiments will also be described in this chapter.

The experimental setup is presented in section 3.2. Details about how the hardware was setup for the first stage of the experiment are explained. Also the software employed to automatically collect the data from the experimental setup is presented.

Section 3.3.1 describes the composition of the gel-based phantom. The characteristics of the phantom are very important on the interpretation of the results and on the achievement of the project's goals. A more human-like phantom has also been experimented. Ex-vivo pork meat has been used as a simulation of the human tissue and the procedures employed for its analysis during the experiments will be addressed on Section 3.3.2.

3.2 Instrumental setup

The experiments developed for this thesis were composed by two main sections, the hardware and the software. Both play a key role on this case study; therefore they will be described bellow.

3.2.1 Hardware setup

The heating equipment employed during all experiments was a therapeutic ultrasound device which is typically applied in physiotherapy. The equipment is a Sonopulse

Generation 2000 device (Ibramed, São Paulo, Brazil). This device includes a transducer with two faces, one with a nominal effective radiation area of 1.0cm^3 and the other with 3.5cm^3. The smaller face allows application of 1 MHz frequencies while the other enables application of 1 and 3 MHz frequencies. Both transducer faces enable application of intensities from 0 to 2W/cm2.

Taking into account practical experimentation it was decided to use the transducer's face with radiation area of 3.5cm^2 and a 1 MHz frequency. All experiments reported on this thesis consider these settings.

The pressure field of the above referred therapeutic ultrasound transducer (TUT) was measured by Dr. Cesar Teixeira [8] in tap water inside a plastic box. The water was at room temperature, around 24º Celsius and the acoustic pressure (Kpa) was measured on points within a distance of 180mm from TUT surface. A 1MHz frequency was applied. The resultant pressure profile along the axis of the transducer is described in figure 3.1.

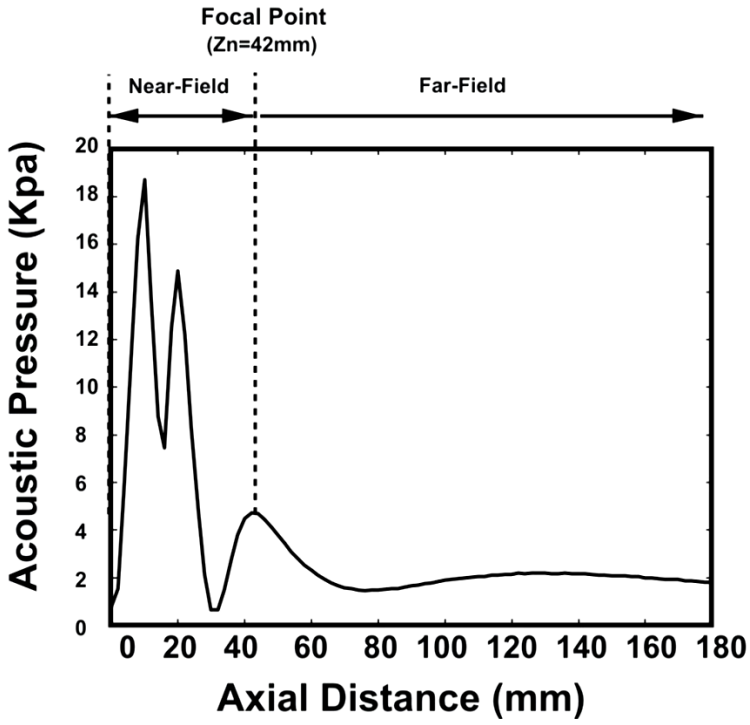

Figure 3.1: Axial pressure characteristics for TUT. [8]

As can be seen from the above figure the transducer's natural focus is at 42mm, this is, the near field length is 42mm. Experiments should therefore consider tissues under analysis at a distance of approximately 42mm from the face of the TUT.

The general setup employed along the several experiments is represented in Figure 3.2.

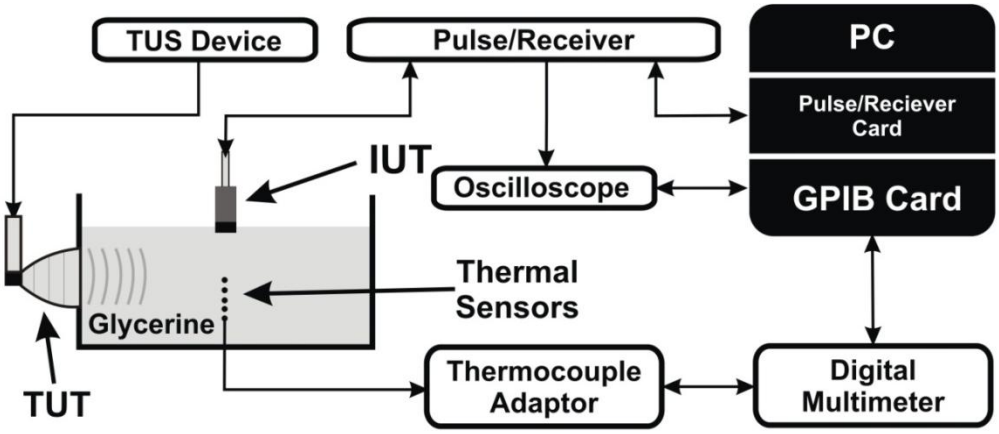

Figure 3.2: Experimental setup used to collect the signals for temperature estimation. [8]

The therapeutic ultrasound transducer (TUT) was from a Sonopulse Ultrasound therapy Device (TUS Device). Two operative modes are possible: continuous and pulsed, the pulsed mode being selected. Frequencies of 1.0 KHz were selected. The temperature inside the phantom was measured by thermocouples Type-k (thermal Sensors), connected to the cold junction compensated. This module amplifies the voltage at the thermocouple terminals and it is connected by a multiplexer board (Keithley, 7700, 20 Chan, Multiplex,USA) to a digital multimeter (Keithley, 2700 Multimeter, USA), which digitalizes the voltage coming from the thermocouples.

In parallel with the temperature data transmission procedure, there is an acoustic intensity signal's acquisition module. These acoustic signals are measured by an imaging ultrasound transducer (IUT) (5 MHz and 7.5 MHz intensities) fed by a pulse/receiver device (Panametrics – NTD, USA) and then transmitted to an oscilloscope device (2024 TDS, Tektronix, USA). The GPIB card ends up on the GPIB bus (National Instruments Co., USA) which acts like a bridge among all measuring devices and the Linux based Machine (Monitoring computer).

Information such as temperature, signal intensity and its shape will be transferred by GPIB bus to a Linux PC (with Debian Operating System) by a dedicated program

developed on Phyton. This application [8] enables analyzing the information provided by all hardware used in this experiment for collecting data.

3.2.2 Software setup

The data acquisition software provide for this study is a high performance data collecting software developed under an open-source license. The acquisition program was written in C and Guile, Perl, PHP, Python ™ and TCL Bindings. It has as bridge connection to all measurement devices and it takes benefit of the Linux-GPIB package. [15]

This software enables monitoring various types of data such as sensors, temperature evolution under graphical representation and produces graphs of the RF backscattered signal.

Temperature monitoring is one of the most important outputs of this software. An example of a possible graph obtained by the software is shown in figure 3.3.

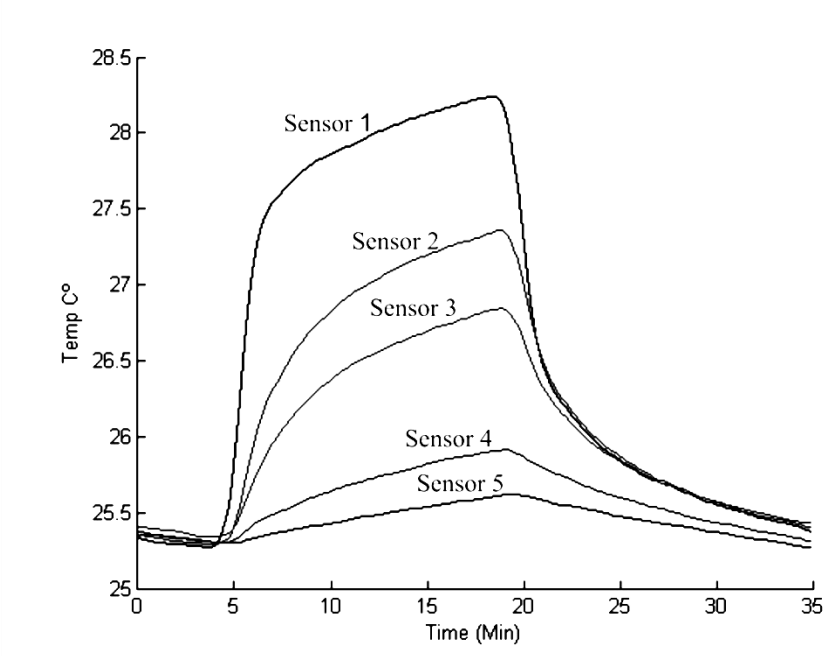

Figure 3.3: Example of a graphical representation produced by the data acquisition software [8] where the temperature of the medium is plotted against time for different sensor locations.

Figure 3.3, presents an example of the temperature variation with time growth for different positions of the sensors. Observing this figure one may conclude that sensor number one presents higher temperature than the others because this sensor is located at the focal point of the therapeutic transducer. By taking into account the other sensor's location and the corresponding temperature curves, it is possible to use this information to calibrate the experimental equipments. [8]

The acquisition software helps us to monitor the data coming from the pulse/receiver device and can also provide us with features to control the instrumental setting such as the damping factor, the energy, the high and low-pass filters and the gain of the ultrasound signals.

Table 3.1 describes the settings employed during the experiments for monitoring the imaging transducer.

Table 3.1: imaging transducer's settings applied during experiments.

Mode	Pulse – Echo
PRF	Trigger/Ext BNC
Energy	100 µj
Damping	250 Ohm
High Pass Filter	1KHz
Low pass Filter	35 MHz
Gain	40 dB

3.3 Phantoms

In this thesis, two types of phantoms were employed. Gel-based phantoms and pork meat phantoms, the following subsections will describe the procedures of developing the experiment for each type of phantom.

3.3.1 Gel-based phantoms

The first experiment developed on this thesis was concerned with the analysis of ultrasound's induced temperature on media when invasive procedures were applied. The media was a simulation of human tissue composed of a gel-based phantom.

In this section, the experiments employing a gel-based phantom will be illustrated by describing the phantom as a structure, the set-up experiment and the procedures taken to collect measurements.

3.3.1.1 Structure

Manufacturing the phantom is one of the most important parts of these experiments. The ability of the phantom to mimic human tissues depends on the phantom's chemical composition and the way it is implemented.

The basic phantom's recipe is based on the work of Sato Et, Al. [16]. In summary the gel-based phantom was created mixing 86% of normal tap (boiled) water with 11% glycerin, 2.5% agar agar and 0.5% graphite for each liter of phantom liquid created. The liquid has to be heated under constant mixing till a homogeneous medium is achieved. The mixture is poured into a plastic box and allowed to cool naturally at room temperature.

Before the phantom was completely solid, five thermocouples were inserted on the phantom in such a way that the thermocouples constitute a line, 5cm apart from the box's face where the therapeutic transducer was introduced. The thermocouples were located equally spaced and regarding that the middle one should be aligned with the middle of the therapeutic transducer's face (figure 3.4). [8]

3.3.1.2 Phantom setting up

The phantom referred on the previous section and represented on figure 3.4 is connected to the rest of the equipment described on Figure 3.2. .

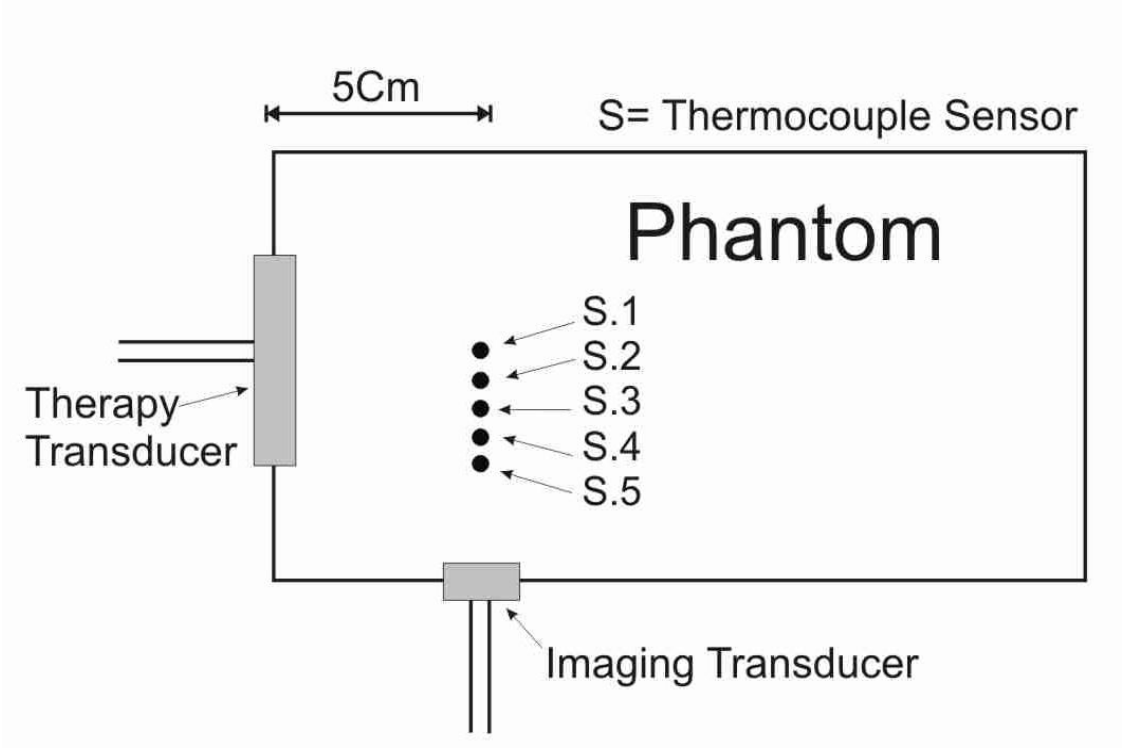

Figure 3.4: Installation of the therapy transducer and the imaging transducer in the gel-based phantom's box and the positioning of the thermocouples (top view).

As mentioned before there are two different types of transducer. One is the imaging transducer which is connected to the pulse/receiver device to monitor the backscattered ultrasound (BSU) signals emitted by the imaging transducer and also the therapeutic transducer which is acting as a heating transducer and is connected to the Sonopulse device.

These two transducers are located on the phantom box at perpendicular positioning, this is making a 90º angle between them (as can be seen in figure 3.4). This perpendicular relation will enable diminishing the scattering effects of the ultrasound waves on the imaging transducer.

Inside the phantom's box the five temperature sensors (thermocouples) enable deterministic measurement of the medium at their locations. They are located in one unique line, vertically aligned with the imaging transducer and with 5mm distance among them to allow five different measuring points inside the phantom [8]. The thermocouples are connected to the multimeter to sense the temperature variation.

3.3.1.3 Measurement procedure

Each experiment lasted for 35 minutes; the first 5 minutes of experiment were just to allow data collection of the initial temperature values of the experiment. Then, during the following 15 minutes, the system was heated. The last 5 minutes correspond to the system cooling at a natural rate. During these 35 minutes the temperature behavior was registered, and during this period data was collected at a rate of one sample in each 5 seconds.

Experiments have been performed employing the therapeutic transducer with energies of 0.5, 1.0, 1.5 and 2.0 W/Cm^2. The heating transducer was set to 1.0 MHz to allow testing different depths of treatment.

The imaging transducer was tested for frequencies of 5 MHz and 7.5 MHz, to avoid any error in sensor positioning and to have more reliable results in terms of the backscatter signal's monitoring.

3.3.2 Pork-meat phantoms

After analyzing the results obtained with the gel-based phantoms decision was made to use more human-like phantoms. Since pork meat, in particular muscle, present very similar properties to real human tissue [8], fresh loin of pork was used as phantom. The loin was sliced into portions of about (3x3x3)Cm. Care has been taken so that loin portions employed for these experiments has not been frozen before the experiment.

3.3.2.1 Phantom setting up

This sub-section describes how the pork loin portion is employed as a phantom on the experiments performed. The pork muscle tissue was placed inside a plastic box and two thermocouples were inserted on the loin as presented on the graphical scheme of Figure 3.5.

Pork muscle tissue, unlike gel-based phantom, has different layers and mainly lipid layers which are asymmetrically distributed in the tissue and consequentially producing

its impact into the backscatter. This feature enables us to consider these experiments as more likely to what happens when ultrasound heating is applied to human muscle.

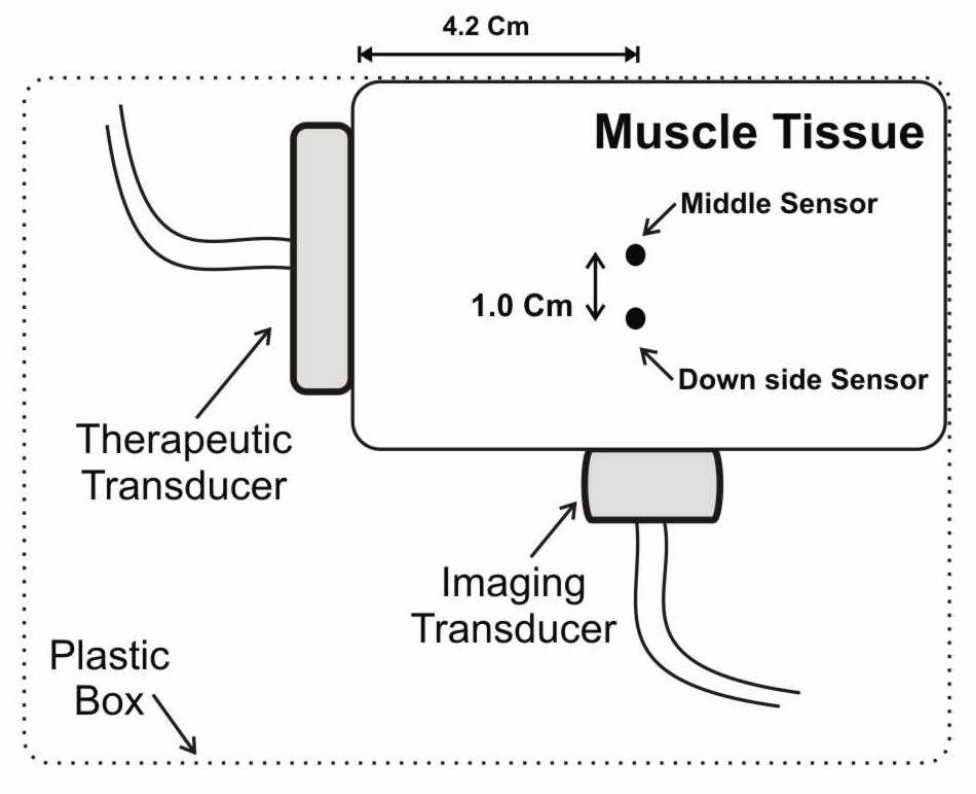

Figure 3.5: Installation of therapy transducer and the imaging transducer when the pork's meat phantom is employed. Location of the thermocouples is also presented (top view).

Similarly to the gel-based phantom experiments two different types of transducers have been used: the imaging transducer (which is connected to the oscilloscope) and the therapy transducer acting as a heating transducer (connected to Sonopulse device).

As before these two transducers are located on the phantom box with a 90º difference in angle, as can be seen in figure 3.5, for the same reason as on the previous experiments.

Inside the pork loin two temperature sensors (thermocouples) have been inserted. They are described as middle and downside sensors in Figure 3.5. These sensors are located in a line 4.2cm apart from the face of the therapy transducer. The line is also vertically aligned with the imaging transducer. The thermocouples are connected to the multimeter to sense the temperature variation. Also each of these temperature sensors has 10mm distance apart from each other to allow measuring temperature at two different points of the phantom.

3.3.2.2 Measurement procedure

Each experiment with the pork-meat phantom took 65min length. The first 5 minutes of the experiments were to allow data collection of the initial temperature values of that particular experiment. During the following 30minutes the system was heated by the therapeutic transducer. The remaining 30minutes correspond to the period where the system was allowed to naturally cool to room temperature. During the 65minutes period data was collected at a rate of one sample in each 5 seconds.

Different experiments have been performed. The heating transducer operated at 1 MHz with energies of 1.0, 1.5, and 2.0 W/cm^2.

The imaging transducer was tested for frequencies of 5.0 and 7.5 MHz.

Chapter 04

Results and Discussions

Chapter 4

Results and Discussions

4.1 Introduction

The results obtained during various experiments and the explanation of the results will be presented.

One of the goals of this thesis is to evaluate how ultrasound-induced tissue temperature evolution relates with BSE variations. To achieve so, the following methodology was taken. The data collected from each experiment was analyzed in terms of graphical and numerical presentations of temperature and ultrasound echoes' data. The different combinations of the ultrasound emitting frequency and energy were tested. Experiments were repeated until scientifically acceptable results were achieved. Furthermore, the pre-selected results were Fourier transformed to enable performing back-scattered energy analysis and to present its relation with the phantom's temperature.

All calculations and plots were performed by Matlab® version 7.1.0.246 (R14) Service pack 3 August 02, 2005.

4.2 Gel-Base phantom analysis

The results hereby presented correspond to the gel-based phantom experiments. Analysis of their behavior under the different experimental setting is also described. The relationships between time, temperature and BSE variations are presented and discussed.

4.2.1 Temperature variation versus time Analysis

For each intensity signal, the relevant temperature at each thermocouple and the echoes received by the image transducer were collected during the whole period of the experiments.

Following the experiment setup described in figure3.4, one of the results obtained to demonstrate the relation between time and temperature, when 0.5 W has been applied with 1 MHz ultrasound signal beam is presented in Figure 4.1. The temperature variation recorded for each thermocouple is identified by the label ‘sensor’ corresponding to each of the five thermocouples.

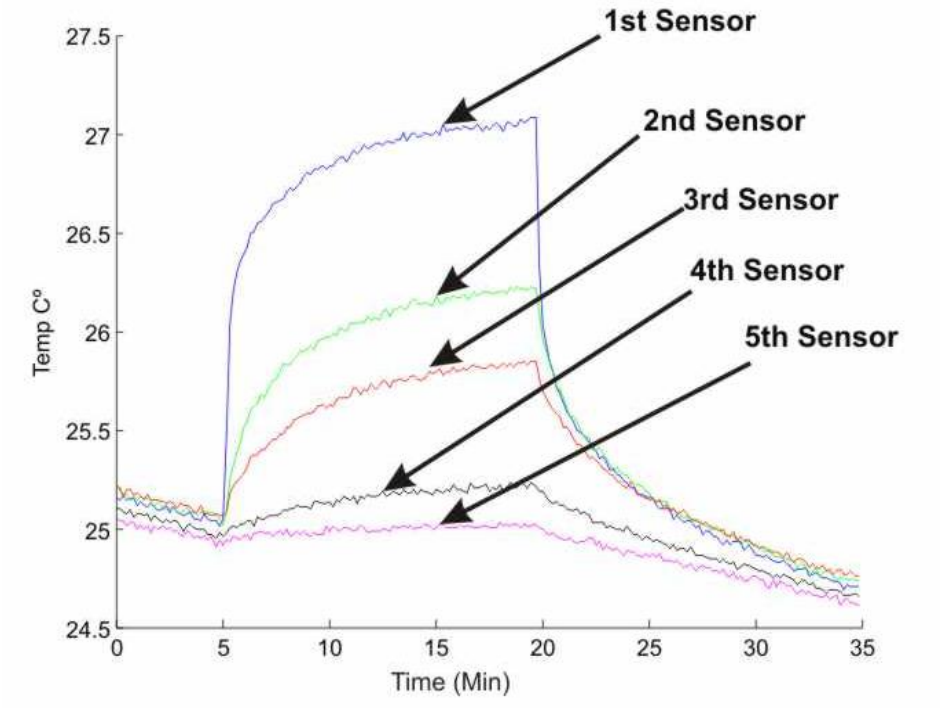

Figure 4.1: Temperature measurement over the time of the experience (35 min) when 0.5 W power intensity and signal frequency of 1 MHz were employed. Labels ‘#sensor’ correspond to thermocouple ‘S#’ in Figure 3.4.

As it can be seen in Figure 4.1 the first sensor presented the highest temperature because it is faced with the focal area of the therapy transducer receiving as so the most intensive signal intensity. On the other hand, sensor number 5 (S.5 in the Figure 3.4) is sensing much less than the first sensor, since it is the most further away from the focal position of the heating transducer. Sensors 2, 3 and 4, located progressively distanced from the centre of the heating transducer (as seen in Figure 3.4) sense temperature progressively less, respectively.

The temperature behavior at each sensor observed in Figure 4.1 is justified by their relative locations to the center of the heating transducer's face. It has also to been taken into account that the sensors are located on a line with 50mm distance from the face of the transducer, This is, they are located at the near field of the transducer (as seen in Figure 3.1).

4.2.2 BSU signal spectrum versus time

In the next step in this experiment, the aim is to monitor the behavior of the echoes. During the phantom's different scattering of signal intensities. Figure 4.2 presents the obtained results.

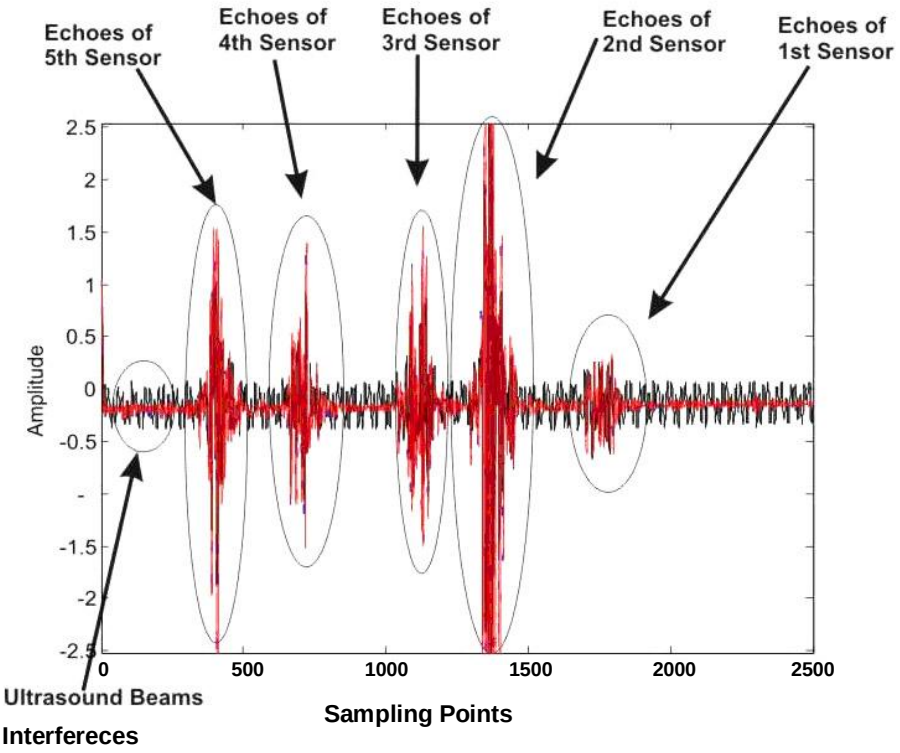

Figure 4.2: The echoes produced by the five sensors and received by the imaging transducer. Sensors numbering is according to figure 4.2, experimental setup was 0.5 Watts of power intensity and a signal frequency of 1 MHz was employed, during 35 min.

Figure 4.2 has a main role in terms of sensor positioning. Further it is relevant for calculation and estimation of temperature by BSE variation. The details presented in this

graph, are used to produce all other data in this case study, to be explained in the next sections of this chapter.

It is important to distinguish red and black waves in Figure 4.2, representing the back-scattered echoes sensed by the imaging transducer. The black color waves are representing the back-scattered signal shape when employing the therapeutic transducer while the red waves show the echoes produced by the imaging transducer.

It is important to mention that, the X-axis in figure 4.2 is expressed as samples. This particular experiment took 35 minutes being collected 2500 samples.

By considering sensor's number in figure 4.2, it is possible to demonstrate the right positioning of the sensors during this experiment. For example sensor number 5 is the closest to the imaging transducer and sensor number 1 is the most distanced one from the imaging transducer. Also by comparison of these results with the temperature results obtained in figure 4.1, one can see that the sensor's placement and temperature are matching.

Figure 4.2 revealed to be very important on the understanding of the combined action of two ultrasound signals in a medium; the ultrasound signal produced by the therapeutic device (the red colored line in figure 4.2) and the ultrasound signal produced by imaging the transducer (the black colored line in figure 4.2).

The observed relationships were taken into account on the following experiences, particularly when analyzing the cooling phenomena and the initial part of the experiments.

4.2.3 US signal echoes shift versus time analysis

As a next step, we concentrated on the echoes received from the imaging transducer. If we consider only one sensor, let us say sensor 1, and observe the echoes returning before the heating transducer is turned on – 1^{st} stage, during heating – 2^{nd} stage, and after the heating transducer has been switched off, this is the cooling period – 3^{rd} stage, one can observe the time-displacement of this echoes for a particular time-slice (from 1695 to 1735 sampling points) in figure 4.3. The data represented in this figure corresponds to experience time instants of 5^{th}, 15^{th} and 25^{th} minutes respectively.

By looking at figure 4.3 it is obvious that during the heating period (stages) the speed of echoes is higher, because of the higher temperature of the phantom (sound waves can travel through phantom faster) leading to echo arrival sooner than in stage 1. During the period where there is no ultrasound beam created by the therapy transducer there is less speed of echoes inside the phantom [17], creating curves with lower amplitudes.

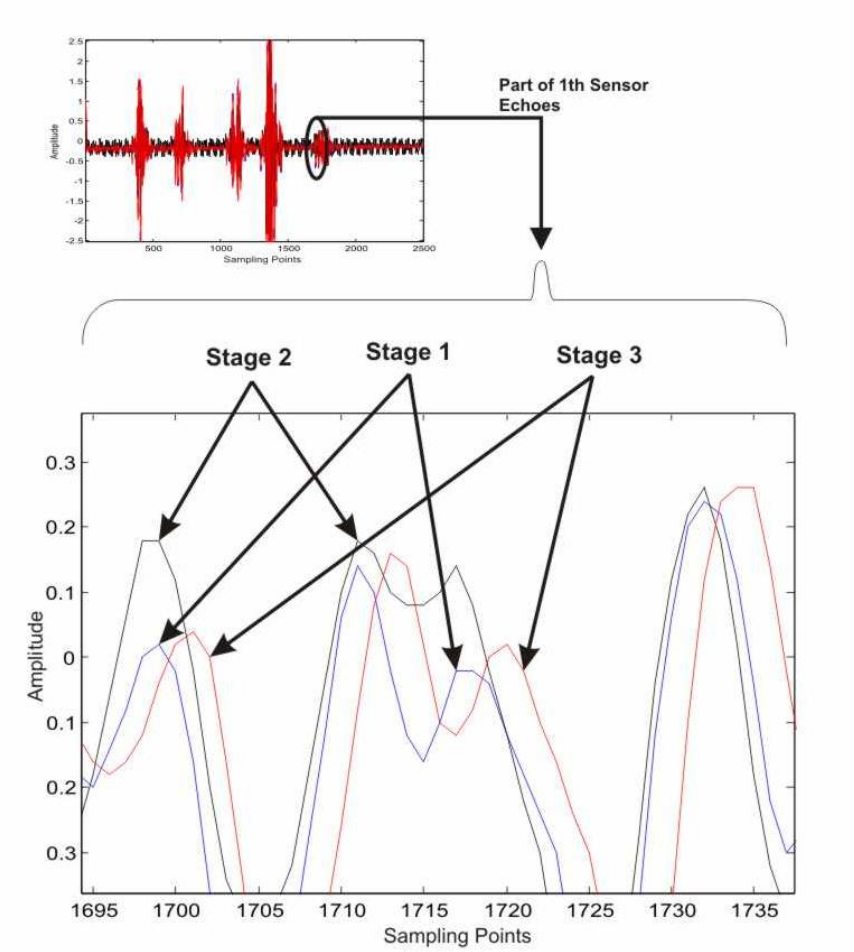

Figure 4.3: Observing the imaging transducer echoes for 1695 to 1735 sampling points, at 5th, 15th and 25th minutes of the experience identified as stage 1, stage 2 (medium being heated by the therapeutic transducer) and stage 3 respectively. Experimental conditions were 0.5 watts of power intensity and a signal frequency of 1MHz within a 35 min period.

In this part, the echo-shifts variation has been analyzed aiming to understand how the echoes amplitude would vary. The echo-shifts estimated for each sensor inside the phantom are presented in figure 4.4. Due to the fact that thermocouples are placed at

different distances from the imaging transducer it is expected that echoes for the closest sensor (sensor 5) would arrive sooner than from the most distant sensor which is sensor 1, there is more delay on echoes coming from sensor number 1 than on echoes of sensor number 5 (which is the closest to the imaging transducer).

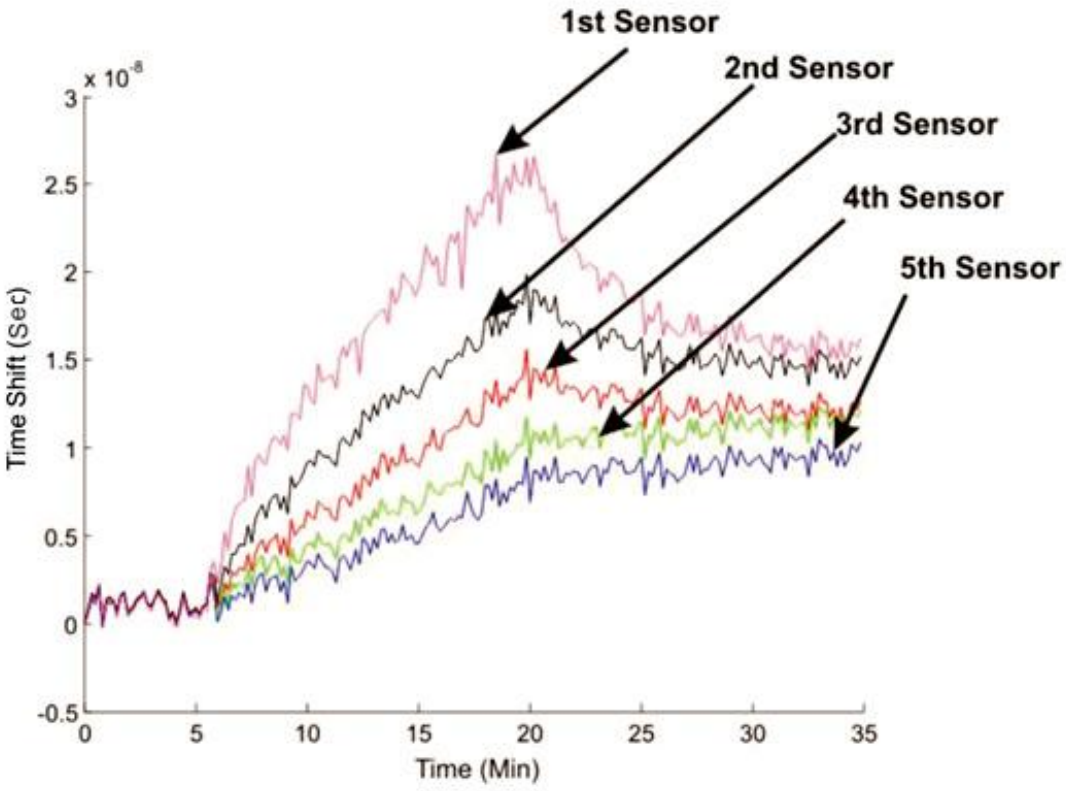

Figure 4.4: Echoes shifts of each sensor inside the phantom. Experimental conditions are 0.5 watts of power intensity, signal frequency of 1 MHz during 35 min period (sensors numbering is the same as in figure 3.4).

Behavior of the time delays of the echoes is directly related to the intensity signal, the distance of the sensors to the imaging transducer and the temperature variation observed at each sensor are in accordance with the results obtained in Figure 4.1.

4.2.4 BSE variation VS time analysis

Now we are going to concentrate on the procedure to calculate the BSE. The echoes provided by the imaging transducer for each sensor were Fourier transformed and based on their spectra, the energy was calculated. [18]

The methodology employed in this experiment for the measurement of BSE from the FFT signal is described in figure 4.5.

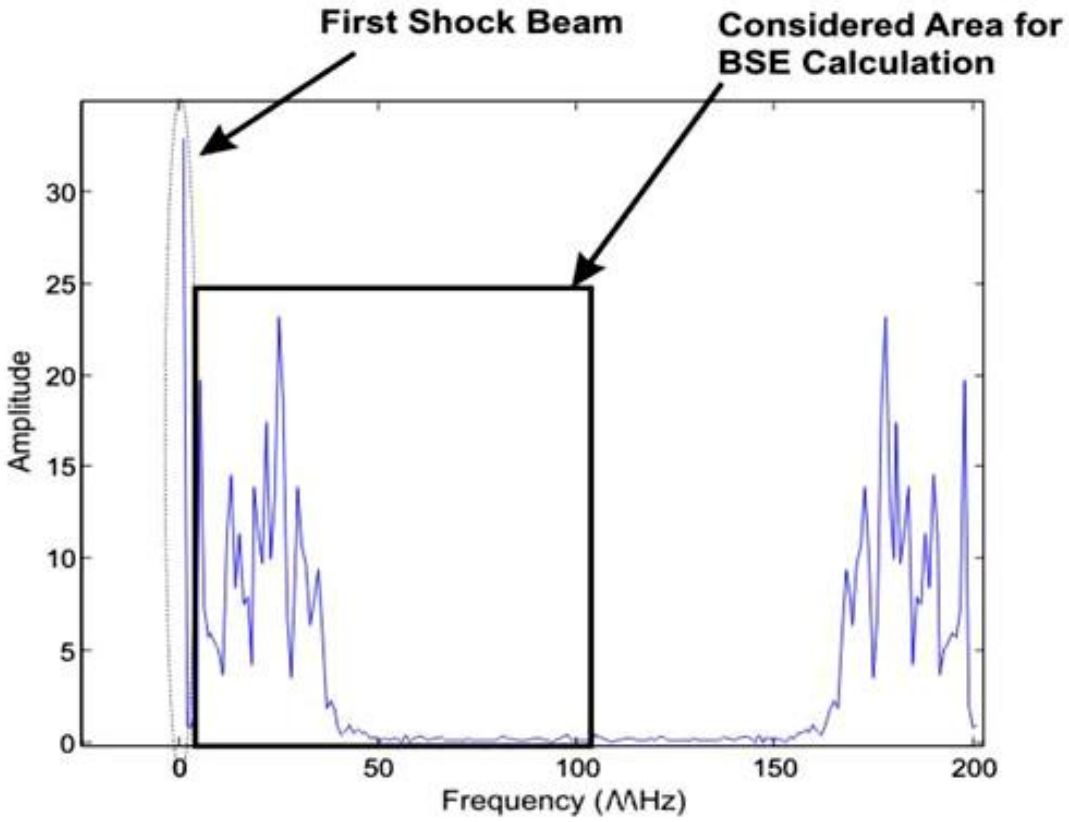

Figure 4.5: Identification of the part of the spectrum used to calculate the BSE of the echoes of sensors. Experimental conditions: 3rd sensor FFT signal, when 0.5 watts of power intensity and signal frequency of 1 MHz is applied. The FFT was computed over 100 points.

The BSE in this experiment was calculated on 50% of the FFT signal, apart from the first 5 samples. These 5 samples correspond to the first ultrasound beam shock (initial ultrasound discharging), which has an enormous peak of energy due to the starting time of the imaging transducer. Therefore this large peak of energy was avoided from the calculations of the BSE's value.

The energy calculation considered three different stages of the experiments: before heating (stage 1), during heating (stage 2) and during cooling (stage 3). These stages were

already represented in Figure 4.3. The idea was to relate the energy of the signals within each stage and then compare the energies among stages.

The BSE calculated for each of these stages and for each sensor is presented on table 4.1.

SENSORS/STAGES	STAGE 1	STAGE 2	STAGE 3
1st Sensor	**0.0805**	**0.0789**	**0.0795**
2nd Sensor	**2.5577**	**1.6016**	**2.5160**
3rd Sensor	**0.4177**	**0.2204**	**0.4015**
4th Sensor	**0.2917**	**0.1652**	**0.2866**
5th Sensor	**0.9629**	**0.5077**	**0.9477**
Total Backscattered energy	**1.0214**	**0.6698**	**1.0214**

* values related to each sensor in this table have coefficient of 1.0E+004 and values related to the total energy of whole signal in different stages have coefficient of 1.0E+006.

Table 4.1: Backscattered energy (BSE) computed for each sensor, at different stages of the experiment and also the total amount of energy in distinct stages. Experimental conditions: 0.5 watts of power intensity, signal frequency of 1 MHz during 35 min period.

As it is shown in table 4.1, the main result is having an equal amount of total BSE in 1st and 3rd stages which demonstrates that the conditions of the experiment were precise, since the energy before and after heating was maintained.

Another key conclusion may be taken by analysis of each sensor individually. For each sensor we can see that the energy is lower during the 2nd stage. Here we can sense the effect of the therapeutic transducer's ultrasound signal with the imaging transducer.

Similar analysis was performed for each sensor but regarding the different power intensities applied during the experiment. We can see from figure 4.6 representing the behavior of the BSE for the 2nd sensor that whatever the intensity applied, the 2nd stage presented always lower BSE values.

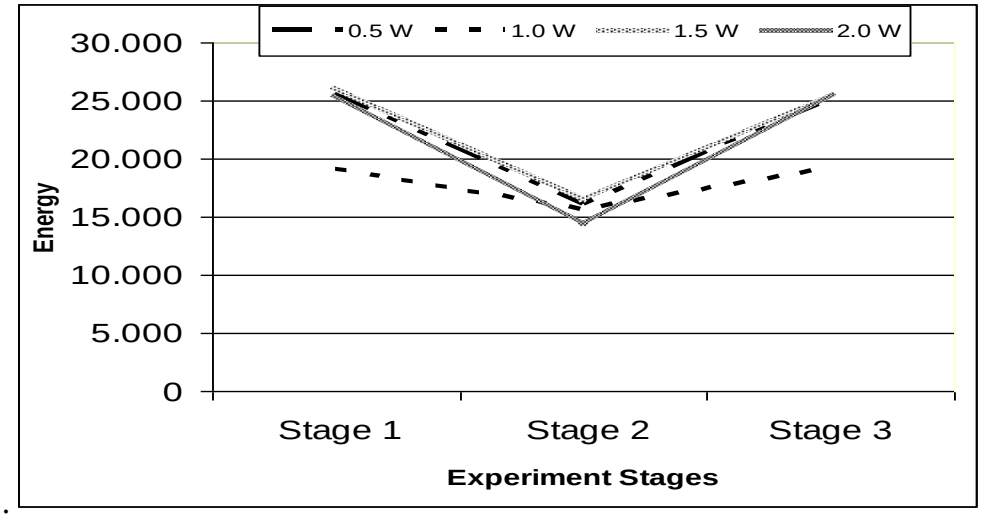

Figure 4.6: Variation of the 2nd sensor BSE with different power intensities: such as 0.5, 1.0, 1.5 and 2.0 W/cm^2, signal frequency of 1 MHz during different experiment stages.

By analysis of figure 4.6, besides the above referred interference between the therapeutic and the imaging transducer, during stage 2 we cannot identify a clear relation between the applied ultrasound energy and the measured energy. [19]

Finally figure 4.7 represents the BSE variation (on logarithmic scale) of sensor 1 during the heating stage.

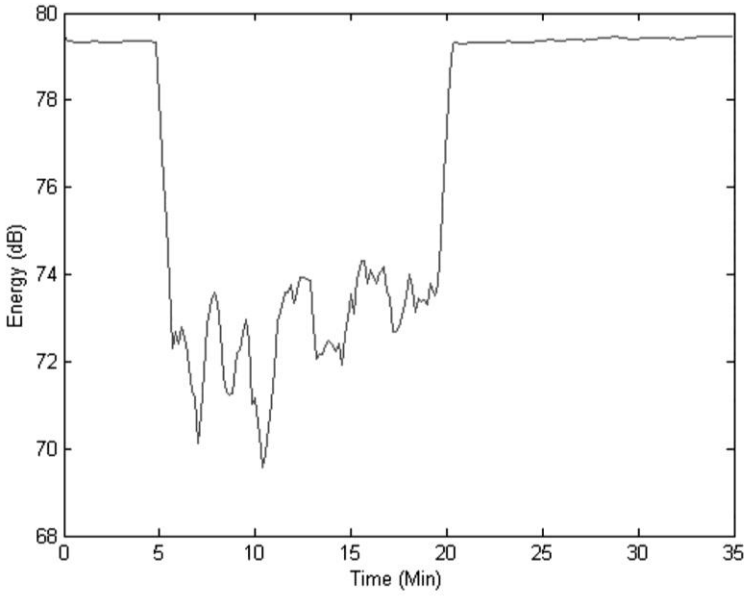

Figure 4.7: BSE variation (logarithmic scale) for sensor 1, experimental conditions: 1.5 watts of power intensity, signal frequency of 1 MHz during the 35 min period of the heating stages.

From figure 4.5, we can see that the shape of BSE variation in the second stage (between fifth and twentieth minutes) of the experiment is completely nonlinear and it has high amount of fluctuations. This quantity of fluctuation makes it extremely difficult to have an effective relation between the BSE and the temperature, which is the goal of this case study.

Generally, the gel based phantom resembles similarly to human tissue in, being characterized by the equation (6).

$$\frac{\eta(T)}{\eta(37)} = \frac{\left(\frac{\rho_m c(T)_m^2 - \rho_s c(T)_s^2}{\rho_s c(T)_s^2}\right) + \frac{1}{3}\left(\frac{\rho_s - 3\rho_m}{2\rho_s + \rho_m}\right)^2}{\left(\frac{\rho_m c(37)_m^2 - \rho_s c(37)_s^2}{\rho_s c(37)_s^2}\right) + \frac{1}{3}\left(\frac{\rho_s - 3\rho_m}{2\rho_s + \rho_m}\right)^2} \quad (6)$$

In equation (6) the change in backscattered energy as a function of temperature for a single scatter can be approximated as the ratio of the temperature-dependent backscatter coefficients η (T), at temperature T and the reference temperature, 37°C (Straube and Arthur 1994) [20]. Where ρ represents the mass density, c(T) is the temperature-dependent speed of sound, and subscripts s and m represent the scattered and medium, respectively. The equation (6) was written in terms of density and speed of sound to allow using measurements of the temperature dependence from the literature. [19]

As a result of equation (6), the BSE should increase during the combination of imaging and therapeutic transducer ultrasound signals, which are completely unlike to the results presented in figure 4.5. Due to this fact the experiment demonstrate that the gel-based phantom mentioned in chapter 3 cannot be employed for temperature estimation by BSE variation.

For the above stated reasons, study will follow by testing a more human like tissue, by using the pork loin muscle as phantom.

4.3 Muscle tissue analysis

The pork loin muscle has similar behavior as the human muscle under the ultrasound beam. Experimental setup was done in the same manner as described in section 4.2.

In this phase of the case study, comparisons play a key role towards the final considerations of this thesis considering temperature estimation by BSE variation. Results obtained in section 4.2 and 4.3 will be compared. To be mentioned that experimenting fresh pork loin, although ex-vivo, will face various restrictions and disturbances, similarly to in-vivo experiments.

4.3.1 Time versus temperature analysis

Sensor's temperature variation is one of the vital keys to assure the properness of sensors' setup and measurement. Unlike section 4.2.1, in this section the experiment duration took 65 minutes to provide a significant range of temperatures and more BSE values.

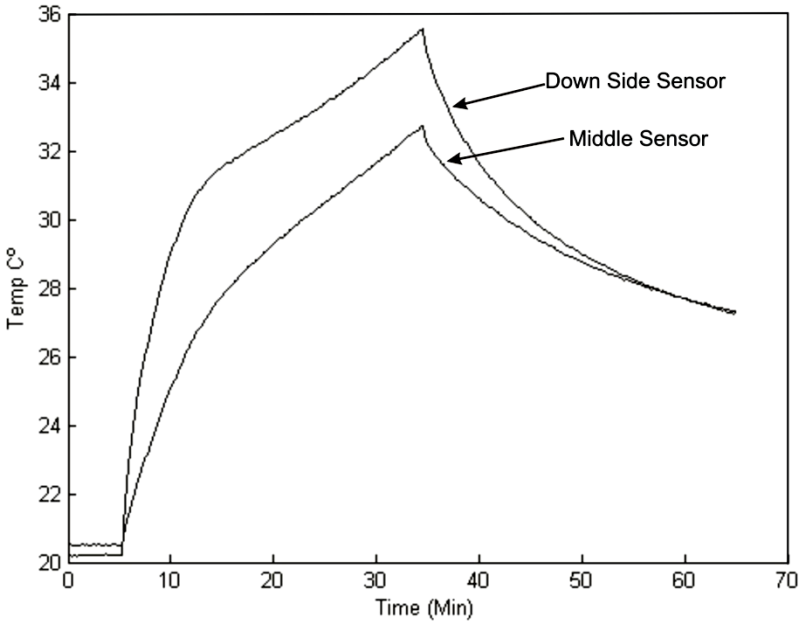

Figure 4.8: Temperature measurement sample for 1.5 watt power intensity and signal frequency of 1 MHz during 65 min. Sensors are named middle and down side, as it is presented in figure 3.5.

In figure 4.8, the behavior of the sensors in terms of temperature variation is almost similar to figure 4.1, even with the increased duration of the experiment. When compared with the curves obtained for the gel-based phantom we can notice a different behavior in

the rising shape of these curves. Also the temperature is growing faster in the gel-base phantom than in muscle tissue. This is due to the purity characteristic of the gel-based phantom. As mentioned before in muscle tissue, there are several layers of other molecules (such as fat) which make resistivity against ultrasound beam and somehow constitute an obstacle to the ultrasound emitting inside the tissue.

4.3.2 BSUsignal spectrum versus time analysis

As in previous section 4.2, echo monitoring was the first approach taken, as it is shown in figure 4.7. Also it is worth to mention that, in this case study the echoes just focused in two sensors for measurements.

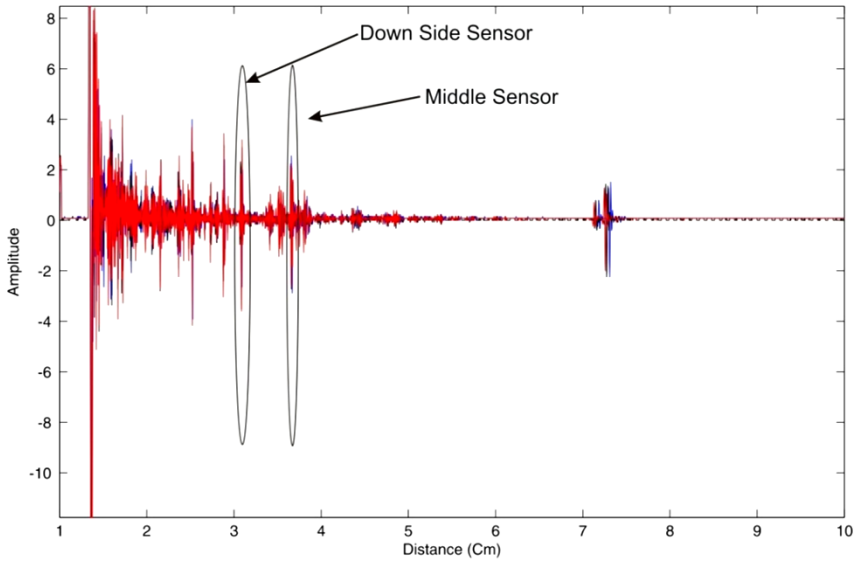

Figure 4.9: The echoes produced by the two sensors and received by the imaging transducer. Sensors are named middle and down side as it presented in figure 3.5. Experimental setup was 1.5 watts of power intensity and a signal frequency of 1 MHz was applied during 65 min.

As it is shown in figure 4.9, there are two sensors in this graphical presentation of ultrasound echoes but unlike the gel-base phantom there is a high amount of the unknown signal peaks in this ultrasound beam monitoring which is mainly produced by different layers of fat and other kind of tissues inside the muscle tissue. Also on the surface of tissue in figure 4.9, there is a massive amount of backscattering caused by the irregular

surface of the tissue. There are also backscattering points which have similar shapes to the sensors backscattering point, so determination of sensor placement turns to be not a simple task as in the case of the gel-based phantom. In this experiment the positioning recognition of sensors was done by moving the sensors inside the tissue and sensing those movements by naked eye inside the oscilloscope device monitor. This action should be done for several times to have an exact identification of the sensors on graphs similar to figure 4.9.

The main restriction for having repeatability of experiments of muscle tissue is the fact that the tissue can only be used once or maximum twice because after the second usage the result in the monitoring of echoes shows some movement regarding the position of the sensors and it disturbs measurements in term of energy. This is because the pork loin has altered due to the heating that it had to be subject to.

4.3.3 BSE variation versus time analysis

By employing a similar procedure as in section 4.2.4, this is, performing the FFT transform of each sensor and calculating the BSE value of each point in the whole duration of an experiment, the result ended up in figure 4.10.

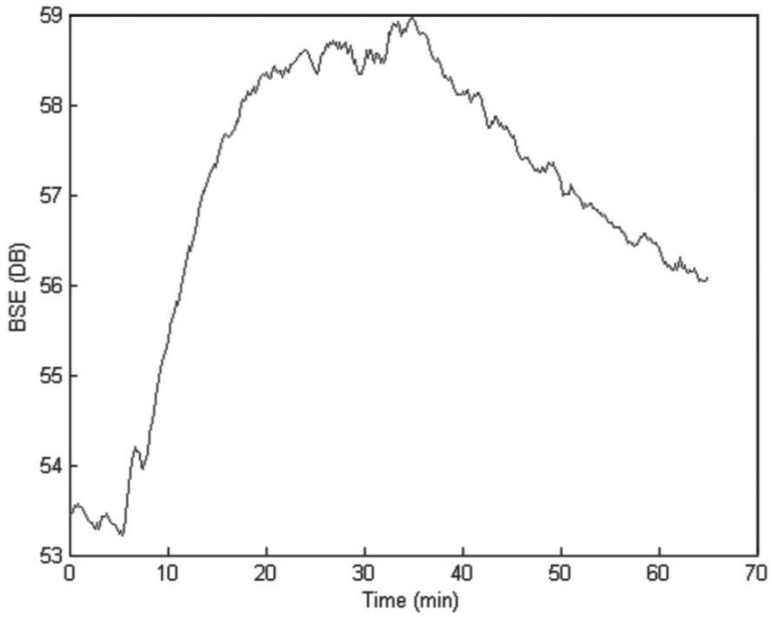

Figure 4.10: BSE (in dB) variation from frequency domain transformation of the middle sensor echoes. Experimental conditions: 1.5 watts of power intensity, signal frequency of 1 MHz during 65 min period.

Unlike the gel-based phantom's BSE variation, in muscle tissue the BSE value is increasing during the heating phase. Also one can testify the sensitivity of the tissue to the ultrasound induced temperature by analyzing Figure 4.8. When the therapeutic ultrasound is switched off (cooling stage) the energy decreases.

When the experiences were repeated using higher energies it was observed that the BSE presented more intensive increasing curves.

4.3.4 BSE variation versus temperature analysis

If we analyze in detail the data presented in figure 4.8 for the slice of time correspondent to the heating process and express BSE against temperature we would have a curve like the one in figure 4.11.

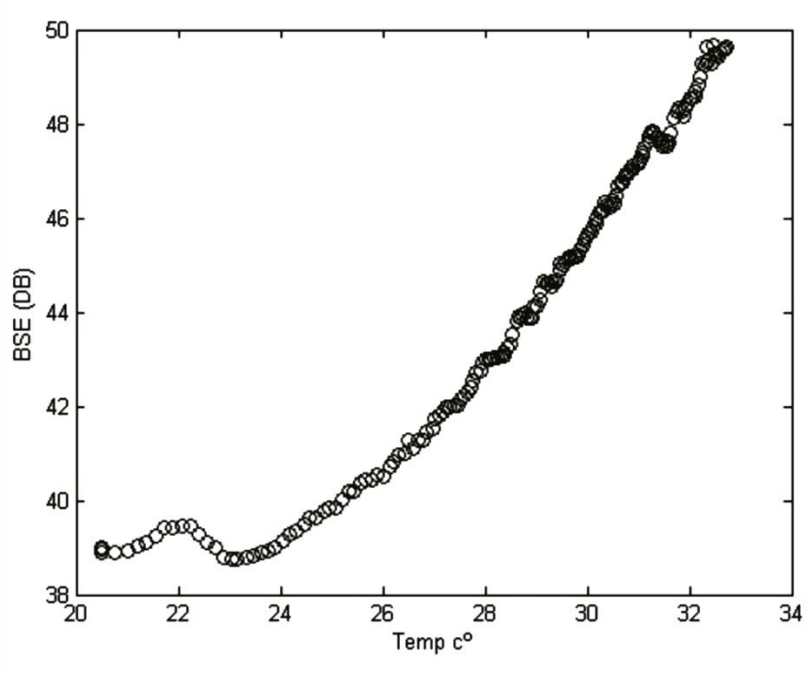

Figure 4.11: The BSE (in dB) variation of the middle sensor echoes versus temperature during the first 35min of a 65 min experiment. Experimental conditions: 1.5 watts of power intensity, signal frequency of 1 MHz during 65 min period.

Different signal power intensities have been tested to establish similar relationships between the BSE variation and temperature. From the analysis of those graphs it is

concluded that temperature estimation inside tissues is possible through the analysis of BSE variations.

To be also mentioned that the curve repeated in figure 4.11 is not a smooth increasing curve. This is due to impurities in the phantom

The rise time of this curve corresponds to 35 minutes of the curve in figure 4.10. If we increased the experimental time, maintaining the phantom's heating, we could achieve higher phantom's temperatures and the existence of more data would enable more suitable estimates for hyperthermia purposes.

4.4 Echo shift analysis in pork muscle tissue

Following subsection 4.2.1 which was focused on gel-based phantom echo shifts, now the pork muscle results are expressed in terms of echo shift as may be seem in figure 4.12.

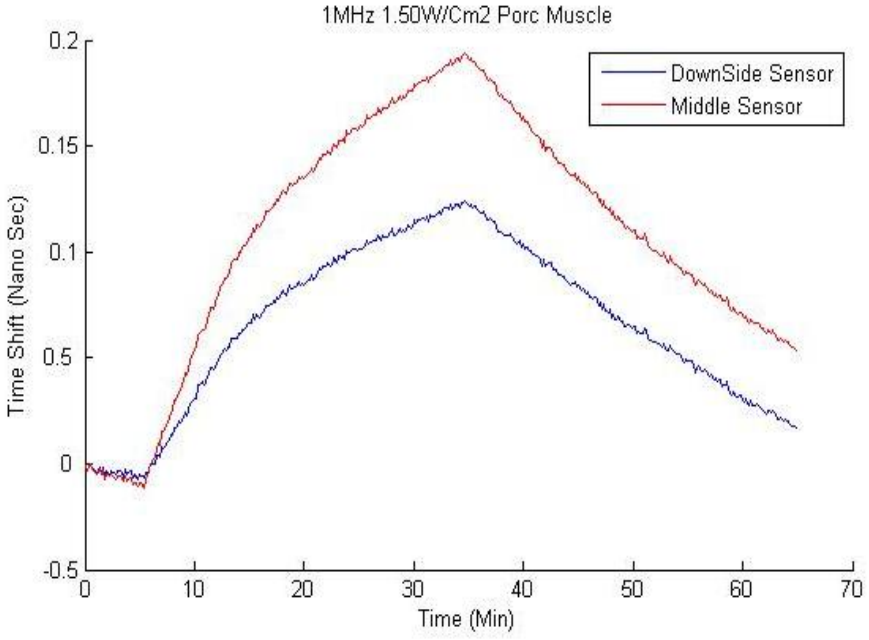

Figure 4.12: Time shifts of each sensor inside the pork muscle tissue. Experimental conditions are 1.5 watts of power intensity, signal frequency of 1 MHz during a 65 min period.

The behavior of the curve is similar to the one representing the sensor in the focal point expressed in figure 4.4. Figure 4.13 represents the relationship between temperature and the time shifts during the whole experimental time (left graph) and only the heating phase of the experiment (right graph).

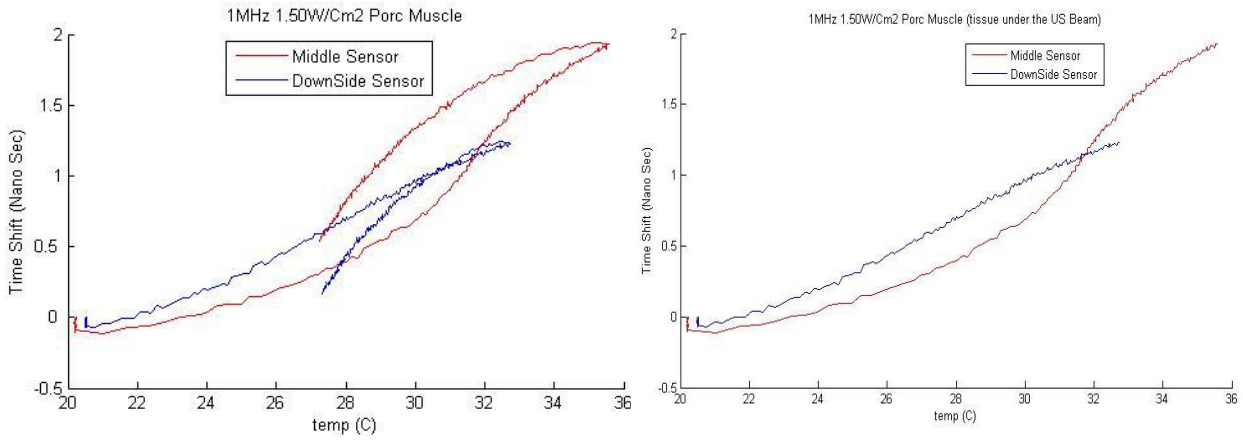

(a) (b)

Figure 4.13: Time shifts versus temperature of each sensor inside the pork muscle tissue. Figure (a) is representing the whole period of the experiment and (b) is focused only on the stage of the experiment corresponding to the heating process. The Experimental conditions are 1.5 watts of power intensity, signal frequency of 1 MHz during 65 min period.

Following the ideas expressed in subsection 4.3.4 we can conclude that the curve related to the sensor in the focal location of the therapeutic transducer (identified in figure 4.13 as middle sensor) is having more time shift during the heating process, and the sensor which is far from the focal point is having less time shifts. According to the conclusions drawn from figure 4.9, we can conclude that it is possible to produce no-linear temperature estimates from the time shifts.

4.5 Experiment Perspective

At the end of this chapter it is necessary to mention some of the main practical issues: experimenting on fresh ex-vivo tissues present higher percentage of risks in the prototype

performance; these risks come out from conditions like: not having proper results in case of any movement of tissue, and also the fact that the experiment is not repeatable unless a chemical stabilizer is used since the tissue's functionality decreases.

Also all experiments reported on this thesis were performed with 1 MHz heating transducer's frequency. However the 3 MHz operating mode of the therapeutic device has also been tested. The results obtained include much incongruence therefore they were not included on this thesis.

By comparison of the behavior of both phantoms described in this chapter, it is possible to extract the fact that, the proposed recipe for gel-based phantom which is mentioned in S. Y. Sato's article [16] should not be used for backscattered energy and temperature relationship studies. For these kind of studies the most realistic and practical approach is to employ the pork meat as phantom due to its human like tissue characteristics as mentioned in section 4.3.

Chapter 05

Concluding Remarks and Future Works

Chapter 5

Concluding Remarks and Future Works

5.1 Concluding Remarks

The major goal of this project was the development of experiments to prove the existence of temperature changes when tissues are heated by ultrasound while analyzing the backscattered energy. The tissues exploited were homogeneous gel-based phantoms and porcine ex-vivo muscle.

Experiments were developed based on an experimental setup already existent in the laboratory. The therapeutic ultrasound transducer was used in the continuous mode at 1MHz and three different intensities were essayed: 1.0 W/cm^2, 1.5 W/cm^{2}and 2.0 W/cm^2. The imaging ultrasound transducer worked in pulse mode at 5MHz. The experiments with the gel-based phantom were taken during a total of 35min, corresponding to 5 min initial settings storage, the 15min corresponding to the heating phase followed by the last 15min where the phantom is allowed to cool. The same experimental phases were undertaken with the porcine sample but all experiments took a total of 65min where the initial setting of 5min was followed by a 30min period of heating and the other 30min representing the cooling stage.

Analysis of the results obtained proved that for both types of phantoms the temporal echo-shifts were representative of the temperature changes occurred. It was also clear that, for each spatial point, the increase in TUS intensity would produce higher shifts on the temporal echoes. When comparing, at similar operational conditions, the TES curves of both types of phantoms one may conclude that with the porcine phantom the TES curve is much more non-linear than those obtained with the gel-based phantoms. Another important feature to report is the fact that while the gel-based phantoms' temperature would return to its initial values after the cooling stage, the porcine sample would rest at nearly 5ºC above its initial temperature.

In what concerns the backscattered energy analysis, experimental results prove that this feature is not suitable to estimate temperature on the gel-based phantoms employed. However, the backscattered energy curves obtained with the porcine samples demonstrate the rise and decay of the phantom's temperature. Results also prove that the relationship between the backscattered energy and the temperature are very irregular, deserving more investigation to evaluate the major factors contributing to this behavior.

The main results hereby described were summarized an a publication presented at the 5th SOFA International Workshop on Soft Computing Applications (SOFA 2012) held on 22nd-24th August 2012, at Szeged Hungary. An extended version will be published in a Springer-Verlag book entitled "Soft computing applications"[21].

5.2 Future Work

Although analysis of the results obtained in this work left several open questions, some of them seem more suitable to constitute the following research steps:

- This thesis' experiments considered the temperature sensors located in a linear line. To enlarge the temperature information in spatial terms, experiments should be performed considering other sensors' dispositions inside the phantoms and preferably, consider setting up experiments for 3D data measurements.
- The porcine samples should be more explored as phantoms due to their similarity with human tissues. Samples considering more fatness in the muscle, different localization of the thermal sensors to include (under the same experimental conditions) information about temperature behavior at simple muscle and fatness should be essayed. Also the usage of surrounding sample's media should be investigated
- Another consideration is concerned with the experimental time and the temperature rise achieved so far. It would be recommended exploring longer experiments and increasing the temperature of the tissues till hyperthermia limits (42 ~ 45ºC).

Bibliography

[1] R. M. Arthur, W.L. Trobaugh, & E.G. Moros, "Non-Invasive estimation of hyperthermia temperatures with ultrasound", Washington university, Department of Electrical and System Engineering, USA, 2005.

[2] "Ultrasound information", Available online:
"http://www.angelfire.com/nj3/soundweapon/ultrales.htm"

[3] Peter Fish, "Physics and Instrumentation of Diagnostic Medical Ultrasound," University of Wales-Bangor, school of electronics engineering science, pp. 7, 1990, ISBN: 0471 92651 5.

[4]SONAER® and SONOZAP Company, (Sonaer Inc.), New York 11735, Available online: "http://www.sonozap.com/Ultrasonic_Information.pdf"

[5] G. ter Haar, "Therapeutic ultrasound," Eur. J. Ultrasound, vol. 9, no. 1, pp.3–9, 1999.

[6] Ultrasound Basics, available online: ttp://www.cmia.org/images/ultasound_basics.pdf

[7] Dr. G. A. Corner, "Physics of ultrasound," Available Online:
"http://www.4shared.com/get/pNWvig5G/Copy_of_Physics_of_ultrasound.html"

[8] C. A. D. Teixeira, "Soft – Computing techniques applied to artificial tissue temperature estimation," Ph.D. dissertation, UALG, PT, 2008.

[9] Redding, Nicholas J. Estimating the Parameters of the K Distribution in the Intensity Domain [2]. Report DSTO-TR-0839, DSTO Electronics and Surveillance Laboratory, South Australia. p. 60, 1999.

[10] Vinayak Dutt, PhD Thesis: “Statistical Analysis of Ultrasound Echo Envelope”, P:4 . August 1995, available online: : http://ndc.mayo.edu/mayo/research/ultrasound/upload/dutt.pdf

[11] J. Acoust. Soc. Am. and Roberto Maass-Moreno, Christakis A. Damianou, and Narendra T. Sanghvi,”Noninvasive temperature estimation in tissue via ultrasound echo-shifts. Part II. In vitro study” Indiana University School of Medicine, Indianapolis Center for Advanced Research, Indianapolis, Indiana 46202, Volume 100, Issue 4, pp. 2522-2530; (9 pages), 1996.

[12] R. Seip, P. VanBaren, C. A. Cain, and E. S. Ebbini, “Noninvasive real-time multipoint temperature control for ultrasound phased array treatments,” IEEE Trans. Ultrason., Ferroelect., Freq. Contr., vol. 43, no. 6, pp. 1063–1073, 1996.

[13] Satoshi Aida, Kenzo Matsumoto, Ayao Itoh, Yoshinori Suzuki, Kinya Takamizawa, “Ultrasound hyperthermia apparatus,” United patent number: 4,620,546, November 1986.

[14] R. Martin Arthur, William L. Straube, Jared D.Starman and Eduardo Moros, “Noninvasive temperature estimation based on the energy of backscattered ultrasound,” Electronic Signals and Systems Research Laboratory, Department of Electrical engineering Radiation Oncology Center, Department of Radiation Oncology, Washington University in St. Louis, Supported by NIH Grant R21 CA90531, NAHS, Reno20, April 2002.
Available Online: http://www.ese.wustl.edu/~rma/sld.a2_nahsinvtlk.pdf

[15] Linux GPIB Project, “The linux gpib package homepage,” May 2007. Available online: http://linux-gpib.sourceforge.net/

[16] S. Y. Sato, W. C. A. Pereira, C.R. S. Vieira, “Phantom to measure Displayed Dynamic Range at Biomedical Ultrasound Equipments,” Revista Brasileira de Engenharia Biomédica, SBEB, vol.19, no. 3, pp.157-166, December 2003.

[17] Peter J. Kaczkowsku. Seattle WA(US), Ajay Anand Elmsford. NY(US), “Non-Invasive Temperature Estimation Technique For HIFU Therapy Monitoring Using Backscattered Ultrasound”, University of Washington. Seattle. WA, Us Patent No.: US 2007/0106157 A1, Pub. Date: May 10, 2007.

[18] Duhamel, P. and M. Vetterli, "Fast Fourier Transforms: A Tutorial Review and a State of the Art," Signal Processing, Vol. 19, pp. 259-299, April 1990.

[19] Jason W. Trobaugh, R. Martin Arthur, William L. Straube, Eduardo G. Moros, “A Simulation Model or Ultrasonic Temperature Imaging Using Change in Backscattered Energy”, National Institute of Health, Ultrasound Med Biol., 34(2):289-298,2008 February.

[20] Straube W, Arthur R. The temperature dependence of backscattered ultrasonic power normalized for use in hyperthermia. “Ultrasound in Medicine and Biology”; 20:915–922, 1994.

[21] Characterization of Temperature-Dependent Echo-Shifts and Backscattered Energy Induced by Thermal Ultrasound, Maria Graça Ruano, César A. Teixeira, and Javid J. Rahmati, V.E. Balas et al. (Eds.): Soft Computing Applications, AISC 195, Springer-Verlag Berlin Heidelberg, pp. 421–431, 2013.

Appendix I: Abbreviations

BSE	Backscattered Energy
BSU	Backscattered Ultrasound
GPIB	General Purpose Interface Bus
IUT	Imaging Ultrasound Transducer
FFT	Fast Fourier Transform
PSF	Point Spread Function
PC	Personal Computer
SNR	Signal to Noise Ratio
SPTPI	Spatial-peak temporal-peak intensity
TUS	Therapeutic Ultrasound System
TUT	Therapeutic Ultrasound Transducer
US	Ultrasound